**The Dissertation Committee for Sungyong Won Certifies that this is the approved version of the following dissertation:**

# REVERSE GENETICS SYSTEM AND FUNCTION OF NSM PROTEIN OF RIFT VALLEY FEVER VIRUS (FAMILY *BUNYAVIRIDAE*, GENUS *PHLEBOVIRUS*)

**Committee:**

Shinji Makino, Supervisor

C.J. Peters, Co-Supervisor

Thomas K. Hughes

Sankar Mitra

Robert E. Johnston

Dean, Graduate School

# REVERSE GENETICS SYSTEM AND FUNCTION OF NSM PROTEIN OF RIFT VALLEY FEVER VIRUS (FAMILY *BUNYAVIRIDAE*, GENUS *PHLEBOVIRUS*)

**by**

**Sungyong Won, M.S.**

**Dissertation**

Presented to the Faculty of the Graduate School of

The University of Texas Medical Branch

in Partial Fulfillment of the Requirements

for the Degree of

**Doctor of Philosophy**

**The University of Texas Medical Branch**

**December, 2007**

## Dedication


I would like to thank my family for their endless love, support and encouragement. My parents, Yongok Won and Youngsoon Kim, have been a solid foundation for my life, allowing and encouraging me to do whatever I have decided to pursue in my life. My wife, Jungsuk Lee has been a shelter and a faithful friend, and an excellent and lovely mother for our children. My precious two sons, Jonghyun Won and Jongbin Won, have understood and cheered me without any complaints about my limited time for interactions with them. I wish to acknowledge the mentorship of Dr. Young Seek Lee at Hanyang University, who stimulated and inspired me to step into a scientific career.

# Acknowledgements

# REVERSE GENETICS SYSTEM AND FUNCTION OF NSM PROTEIN OF RIFT VALLEY FEVER VIRUS (FAMILY *BUNYAVIRIDAE*, GENUS *PHLEBOVIRUS*)

Publication No._____

Sungyong Won, Ph.D.

The University of Texas Medical Branch, 2007

Supervisor:  Shinji Makino

Rift Valley fever virus (RVFV) (genus *Phlebovirus*, family *Bunyaviridae*) has a tripartite negative-strand genome, causes a mosquito-borne disease that is endemic in sub-Saharan African countries and results in large epidemics among humans and livestock. Furthermore, it has potential as a bioterrorist agent and poses a risk for introduction to other areas. In spite of its danger, neither veterinary nor human vaccines are available. I established a T7 RNA polymerase-based reverse genetics system to rescue infectious clones of RVFV MP-12 strain entirely from cDNA, the first for any phleboviruses. Using this system, RVFV carrying substitution mutations of the M gene preglycoprotein region (pre-Gn region), one lacking NSm protein expression, one lacking 78-kDa protein expression, and one lacking expression of both proteins, were rescued and compared in cell culture. All of the mutants and their parent virus produced plaques with

similar sizes and morphologies in Vero E6 cells and had similar growth kinetics in Vero, C6/36, and MRC5 cells, demonstrating that the NSm and 78-kDa proteins were not needed for the virus to replicate efficiently in cell culture. A competition-propagation assay revealed that the parental virus was slightly more fit than the mutant virus lacking expression of both proteins. To determine the biological functions of the NSm and 78-kDa proteins, I generated the mutant virus, arMP-12-del21/384, carrying a large deletion in the pre-Gn region of the M segment. Neither NSm nor the 78-kDa proteins were synthesized in arMP-12-del21/384-infected cells. Although arMP-del21/384 and its parental arMP-12 showed similar virus growth kinetics, viral RNA, and proteins accumulation in infected cells, arMP-12-del21/384 infection induced extensive cell death and produced larger plaques than did the arMP-12 infection. arMP-12-del21/384 replication triggered apoptosis, including caspase-3 activation, cleavage of its downstream substrate, poly-ADP-ribose polymerase, and activation of initiator caspases, caspase-8 and -9, early in infection as compared with arMP-12 replication. NSm expression in arMP-12-del21/384-infected cells suppressed the severity of caspase-3 activation. Further, NSm protein expression inhibited staurosporine-induced activation of caspase-8 and -9, demonstrating that other viral proteins were dispensable for the NSm's function in inhibiting apoptosis. RVFV NSm protein is the first identified Phleobovirus protein that has antiapoptotic function.

# Table of Contents

# List of Tables

# List of Figures

# List of Illustrations

# Chapter 1:  General Introduction

## I. THE BUNYAVIRIDAE

### Classification

The family *Bunyaviridae*, which was formally established in 1975 (38), currently contains four genera of animal-infecting viruses (*Orthobunyavirus, Phlebovirus, Hantavirus,* and *Nairovirus* genera) and one genus of plant-infecting viruses (*Tospovirus* genus), based on their serological, biochemical, and genetic relationships (109).  Most viruses in the family have been isolated from or are transmitted by arthropods, primarily, mosquitoes, ticks, sand flies, or thrips, except for Hantaviruses that are rodent-borne and are transmitted through aerosolized rodent excreta (109).

The largest genus in the family is the *Orthbunyavirus* genus with 49 species including Bunyamwera virus and California encephalitis virus, and 3 tentative species. The *Hantavirus* genus has 22 species with Hantaan virus and Sin Nombre virus, and the *Nairovirus* genus includes 7 species with Crimean-Congo hemorrhagic fever virus. In the *Phlebovirus* genus, thus far, 9 species including Rift Valley fever virus and Uukuniemi virus and 16 ungrouped viruses are reported. Also 7 species and 8 tentative species have been classified in the *Tospovirus* genus (1).  In addition, there are 7 groups (19 viruses) and 22 ungrouped viruses that have not been classified to a specific genus in the family *Bunyaviridae*, since no biochemical characterization of the viruses has been reported to determine their taxonomic status (1).

**Genomic structure, organization and coding strategies of viral genes**

Virions in the family have a spherical structure of 80 to 120 nm in diameter. The viral genome is composed of three single-stranded, negative-sense RNA genome segments designated as large (L), medium (M), and small (S). All three segments of a virus have the same complementary nucleotides at their 3' and 5' termini, which are highly conserved among viruses within same genus, but differ from those of viruses in other genera (109). The terminal complementary nucleotides can base-pair forming stable panhandle structures that result in noncovalently closed circular RNAs (52). The nucleocapsid protein (N) of a virus encapsidates individual L, M, and S segments, which generates helical structures (109). For infectivity, a virion must contain at least one each of the viral-sense L, M, and S RNAs, but it can harbor unequimolar ratios of L, M, and S RNAs (129), which may be responsible for the different size of virions estimated by electron microscopy. In addition to viral-sense RNA (vRNA), small amounts of complementary-sense (cRNA) of their segments can be incorporated into a virion of some viruses in the *Phlebovirus* and *Tospovirus* genera (56, 70, 116), suggesting that their gene products play a role in early replication events (56).

It has been known that there are both similarities and differences in the coding strategies of viruses in the family *Bunyaviridae*. Viruses in the family encode all structural proteins (nucleocapsid protein: N, envelope glycoproteins: Gn and Gc, and RNA-dependent-RNA-polymerase: L) in virus (cRNA). Thus far, phleboviruses and orthobunyaviruses encode nonstructural proteins (NSm) from the M segment cRNA, and orthobunyaviruses encodes another nonstructural protein (NSs) from the S segment cRNA. Interestingly, phleboviruses encode a nonstructural protein (NSs) from their S segment, and tospoviruses encode nonstructural proteins, NSm and NSs, from their M

and S segments, respectively, by an ambisense strategy; these genes are encoded from subgenomic mRNAs of the same polarity as vRNAs. Therefore, vial gene coding strategies of orthobunyaviruses, hantaviruses and nairoviruses follow strictly negative-sense coding strategies, whereas phleboviruses and tospoviruses use ambisense coding strategies for their nonstructural proteins (109).

**General cycle of replication and viral gene products**

The general cycle of the replication process for viruses in the family *Bunyaviridae* starts with viral attachment to the host cells. The mechanisms that viruses of the family utilize for access to the host cell's cytoplasm appear similar to those reported for many other enveloped viruses. In the initial step, viral envelope glycoproteins, Gn and/or Gc interacts with cell surface receptors, although major host cellular receptors have not been identified for most viruses in the family and little is known about the usage of Gn or Gc for attachment. At least, from the fact that both the Gn and Gc proteins of the phleboviruses, Rift Valley fever virus (64), and Punta Toro (98) virus, and those of the hantavirus Hantaan virus (5) have neutralizing and hemagglutination-inhibiting sites, it can be speculated that both proteins may play a role in attachment, either directly or indirectly by conformational requirements.

For virus entry, viruses in the family seem to enter via receptor-mediated endocytosis forming coated vesicles, since virus particles of certain genera are observed in phagocytic vesicles right after infection (36). During the uncoating process, like other enveloped viruses, acidification of the endosomes is supposed to trigger a conformational change in Gn and/or Gc that facilitates fusion of the viral and cell membranes allowing access of the viral genome and polymerase to the cytoplasm (109).

Once viral genomes are uncoated, only encapsidated vRNA can be transcribed into mRNA by interaction of the virion-associated polymerase (L) and the three viral RNA templates. During primary transcription, as with influenza viruses, viruses in the family hijack capped oligonucleotides from host mRNAs to use as primers for the transcription by endonuclease activity of the L protein (59, 60). While influenza viruses scavenge primers from newly synthesized mRNAs in the nucleus, viruses in this family take primers from the existing host mRNAs. As a result, mRNAs of the viruses have an extra 10-20 heterogeneous nucleotides at 5' termini that is not observed in vRNA (15).

For the genomic replication of negative-strand viruses, it is required that a switch occurs from mRNA transcription to synthesis of full-length cRNA templates and vRNA. However, the processes involved in switching from primary transcription to genome replication have not been completely identified for any member of the family, even though there is an implication that continuous protein synthesis is essential for replication of the genome (109).

In translation and processing of viral proteins, S and L mRNAs are translated on free ribosomes, and M mRNAs are translated on membrane-bound ribosomes in the endoplasmic reticulum.

The N proteins of viruses in the family are expressed from the S segments ranging from approximately 19-kDa (orthobunyaviruses) to 54-kDa (hantaviruses and nairoviruses) without posttranslational modifications (109). In addition to the N proteins, the S segments of orthobunyaviruses, phleboviruses, and tospoviruses encode NSs proteins, whose sizes range from 10-kDa (orthobunyaviruses) to more than 50-kDa (tospoviruses). There is no solid evidence that the NSs proteins share the same characteristics and functions among different genera or, even, in same the genus.

4

However, expression studies indicated that NSs proteins of orthobunyaviruses promote apopotosis, and/or inhibit cellular translation and RNA synthesis by minigenomes (17, 30, 132), and counteract interferon (IFN) regulatory factor 3-mediated induction of early cell death (67). The NSs protein of Rift Valley fever virus (RVFV) in phleboviruses is known to have an IFN-antagonistic function (20) and inhibits the function of host RNA polymerase II by interacting with the p44 subunit of the TFIIH transcription factor; synthesis of host mRNAs, including that of IFN mRNA, is inhibited in cells expressing NSs proteins (78). In contrast to NSs of orthobunyaviruses, coexpression of RVFV NSs protein with L and N proteins substantially enhances minigenome replication and transcription (54).

The matured viral envelope glycoproteins (Gn and Gc) of most viruses in the family result from host signalase-mediated cleavage of the polyprotein precursors that are translated from a single mRNA species of the M segments (109). All polyprotein precursors of the M segment show variable numbers of putative transmembrane regions, and a membrane anchor region at the carboxyl-terminus, indicating that envelope glycoproteins of viruses in the family *Bunyaviridae* are typical class 1 membrane proteins, with the amino terminus exposed on the surface of the virion and the carboxyl terminus anchored in the membrane (109).

In addition to Gn and Gc, the nonstructural proteins (NSm) of phleboviruses and bunyaviruses are translated from the same mRNA as Gn and Gc. However, their functions have not been identified in spite of the abundance of these proteins in the infected cells. Unlike all other viruses in the family, the NSm protein of tospoviruses is translated from an ambisense mRNA (69), and is involved in cell to cell movement of the nonenveloped ribonucleocapsid structures across the cell walls in infected plants (120).

5

The L proteins of viruses in the family *Bunyaviridae* are produced from the L segments ranging from about 237-kDa (phleboviruses) to 459-kDa (nairoviruses) without known processing or posttranslational modifications (109). Analysis of amino acid sequence reveals several conserved motifs of RNA polymerases and endonucleases, which are confirmed by in vitro expression system of Bunyamwera virus L protein (59, 60).

Unlike other negative-strand RNA viruses, most members of the family *Bunyaviridae* appear to assemble intracellularly by budding at smooth-surface vesicles in the Golgi (109). The tospoviruses also form virions in the Golgi by merging Golgi membranes around the ribonucleocapsids instead of budding (66). However, certain hantanviruses (Sin Nombre and Black Creek Canal viruses) have shown to bud preferentially from the plasma membrane of infected cells (49, 104), and the phleboviruses (Rift Valley fever virus) bud from the plasma membrane as well as from the Golgi of primary rat hepatocytes (4).

Another unique feature of members of the family is that these viruses do not have a matrix (M) protein, bridging the viral envelope proteins and their nuclocapsids and nucleating for assembly. Even though the signal directing the ribonucleocapsids to the budding compartment has not been identified, the absence of the M protein may suggest that there is a direct interaction between the ribonucleocapsids and viral envelope proteins.

After budding into the Golgi cisternae, most probably, virions are transported to the cellular plasma membrane within vesicles via the secretory pathway, and the virions are then released from infected cells by normal exocytosis in which virus-containing vesicles fuse with the cellular plasma membranes, since numerous viruses in the family

6

have been observed late in infection within vesicles or in the process of exocytosis by electron microscopy (4, 104).

## II. RIFT VALLEY FEVER VIRUS

### General features

Rift Valley fever virus (RVFV) belongs to the *Phlebovirus* genus within the family *Bunyaviridae*. Like other members of the family, RVFV has a tripartite single strand RNA genome composed of L, M and S segments. The L and M segments are of negative polarity, while the S segment has an ambisense polarity. The L segment encodes the RNA dependent RNA polymerase (L). The M segment expresses polyprotein precursors that are cleaved into the envelope glycoproteins (Gn and Gc), 78-kDa protein, and a nonstructural protein (NSm) as a result of posttranslational cleavage. The S segment encodes the nucleocapsid protein (N) in cRNA and a nonstructural protein (NSs) in vRNA that are separated by an intergenic region (Illustration 1.1).

As with all negative-strand viruses, the RVFV genome can be transcribed and replicated only when it is a ribonucleocasid complex with N and L. Unlike vRNA and cRNA, viral mRNAs are capped with 5' extensions by cap snatching from host mRNAs, and no poly-(A) tails are found at their 3' ends. Viral open reading frames (ORFs) are flanked by non-coding regions, most probably, harboring critical cis-acting elements for viral transcription, genome replication, encapsidation, and packaging into progeny virions (Illustration 1.1). Also, highly conserved complementary nucleotide sequences are located at the segment ends by which intra-strand base-pairing leads to form circular

RNAs providing the functional promoter region for the interaction of the viral polymerase with the genomic RNA segments.

RVFV are known to bud at smooth surface membranes of the Golgi, and the budding site seems to be determined by a Golgi-retention signal of the glycoproteins (Gn and Gc) at that particular site (46, 48). Since RVFV does not have a matrix protein linking viral envelope glycoproteins (Gn and Gc) and ribonucleocapsids, it is speculated that there is a direct interaction between them.
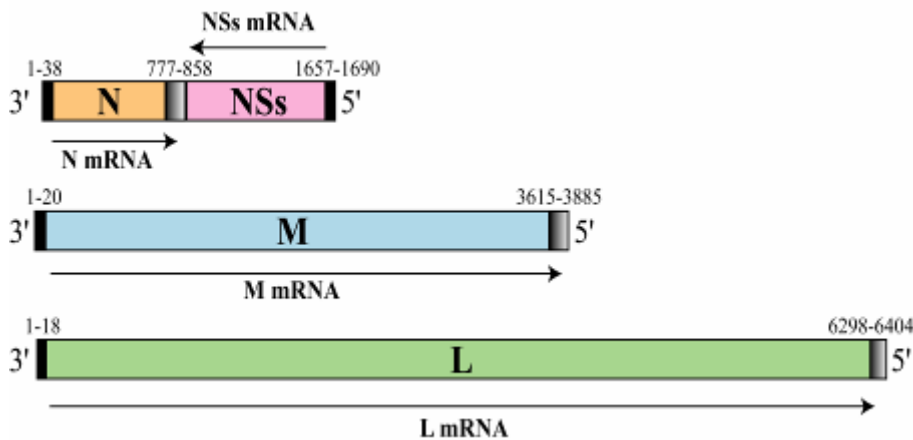


Illustration 1.1: Schematic representation of the genome organization of RVFV

**Transmission**

RVFV causes severe epidemics among ruminants, such as sheep, goats and cattle, in the sub-Saharan area of the African continent, Egypt, Yemen, and Saudi Arabia, and is

8

also recognized as a human pathogen that causes a syndrome of fever and myalgia, a hemorrhagic syndrome, ocular disease, and encephalitis (7).

RVFV is a mosquito-vector borne virus, thus it is normally transmitted by the bite of infected mosquitoes. Incidentally, humans can be infected by contact with infected tissues or aerosols. Numerous strains of RVFV were isolated from various species of mosquitoes captured in the wild (40). Since the virus can be transmitted by an unusually wide range of mosquitoes such as *Aedes, Culex, Anopheles*, and *Eretmapodites*, and livestock can circulate with sufficiently high levels of the virus to infect mosquitoes, many other parts of world would be susceptible to its epidemic transmission (87, 127, 128).

The notable epidemics/epizootics occurred after periods of abnormally heavy rains. One of outbreaks was occurred in 1997-1998 after El Nino/Southern Oscillation (ENSO) floods in East Africa with the epidemic disease activity in Ethiopia, Sudan, Somalia, Kenya and Tanzania, and subsequent introduction of the virus into Yemen and Saudi Arabia (7, 96). The presence of water is one of essential factors for the establishment of mosquito breeding sites. RVFV seems to be maintained in nature between epidemic periods (interepidemic periods) principally by transovarial transmission in mosquitoes with a low level of transmission to livestock, and epidemics are precipitated by unusually heavy rains that lead to an explosive increase in vector populations (81, 135). It is not known whether a vertebrate reservoir for the propagation of the virus exists in nature, or not.

**Pathogenesis**

RVFV had been known as a virus causing an enzootic disease affecting domestic animals, especially sheep, cattle and goats, producing high mortality rates in new-born

animals and abortion in pregnant animals. Only a few fatal human cases were recognized before 1977. In humans, RVFV infection causes a dengue-like illness characterized by fever, headache, often associated with hemorrhages. Also, in some cases, severe complications like retinitis, encephalitis and hepatitis with fatal hemorrhagic fevers are observed (40).

The pathogenesis of RVFV infection includes propagation of the virus from the initial site of replication to critical organs such as spleen, liver and brain, which are damaged by the cytopathic effects of the virus or immunopathological responses. RVFV infection primarily affects the liver with rapid and massive hepatocellular necrosis, lesions of which form scattered primary necrotic foci composed of dense aggregates of cytoplasmic and nuclear debris, and infiltration of neutrophils. Most of the normal architecture of the liver is lost due to massive destruction of hepatocytes. Hemorrhages can be observed in the liver of lambs and sheep, and younger animals seem to be most susceptible (28).

Haemostatic derangement is observed in RVFV infection with a profound leucopedia, elevated serum enzymes associated with severe liver damage, and thrombocytopenia. In the development of the hemorrhagic state, the major lesions are vasculitis and heptatic necrosis (95). Severe liver damage presumably reduces production of coagulation proteins and promotes occurrence of disseminated intravascular coagulopathy and impaired blood flow. Disseminated intravascular coagulation with prolonged bleeding time, prothrombin time, and activated partial thromboplastin time, elevated fibrin degradation products, and decreased fibrinogen has been observed in severe cases (40).

Ocular lesions may occur as a complication of RVFV infection in humans, occasionally appearing at the time of the acute febrile illness with focal retinal ischemia associated with thrombotic occlusion of arterioles and capillaries and characterized by retinal edema and loss of transparency due to dense white exudate and hemorrhages (114, 115). In addition, encephalitis has been observed at one to four weeks after the acute febrile illness in a small proportion of human RVFV-infected patients (97). The virus appears only in the brain at a late stage in rats by which time circulating antibody is already present (3), suggesting that there is an immunopathological basis to the encephalitis as well as the direct cytopathic effects of the virus. Sometimes, suppression of the usual fatal hepatitis by the administration of antibody or interferon, or infection of attenuated RVFV can lead to the development of the late encephalitis (13, 97).

In RVFV infection of pregnant sheep, cattle and goats, abortion is a usual manifestation. Most cases of abortions lead to fetal death with lesions similar to those present in new-born lambs, including extensive hepatic necrosis, while acute abortions may be related to the febrile illness of the pregnant animals. The fetal brain and viscera are also infected, and virus or antigen can usually be detected in them. Placental lesions have not been observed, but it is possible that placentitis leads to the occurrence of abortion since virus can be isolated from the placenta (28, 96, 97).


**Reverse genetics system**

The rescue of recombinant RNA viruses from cloned cDNA (infectious cDNA clone) has provided researchers with a powerful tool to study virus replication and pathogenesis, through genetic manipulation such as point mutations, deletions, insertions, inversion, and translocation of the virus genome using site-directed mutagenesis or PCR-

based cloning strategies. Further, reverse genetics systems can be used for screening antiviral drugs with recombinant viruses containing a reporter gene, or used in vaccine development, especially for the production of attenuated viruses.

The first infectious clone system for a mammalian RNA virus was established for poliovirus, which is a positive-strand virus (103). Subsequently, infectious cDNA clones were generated for a large number of other positive-strand RNA viruses including flaviviruses, by use of the infectious nature of the viral RNA; following transfection of naked genomic RNA into mammalian cells, positive-sense viral RNA genomes can act as mRNA to express all proteins required for the viral replication (106). It had taken almost a decade to establish the first rescue system for a negative-strand RNA virus, influenza A virus (85), where a helper virus was used to provide the viral proteins (e.g. nucleocapsid protein: N, RNA-dependent-RNA polymerase: RdRp). Expression of the viral proteins was needed for transcription and replication of the genome since negative-sense viral RNA genomes are not infectious.

To overcome the difficulties in establishing infectious cDNA clones for negative-strand RNA viruses, an alternative approach, a minigenome system, was developed. In the system, cloned cDNAs were used to express artificial vRNA analogues, which mimic miniature viral genomes consisting of a reporter gene (e.g. chloramphenicol acetyltransferase: CAT, luciferase, green fluorescent protein etc.) flanked by the minimal regulatory sequences at the genome ends (non-coding region: NCR) under the transcriptional control of a promoter such as bacteriophage T7 polymerase. The first entirely plasmid-based approach was dependent on the expression of proteins, which are components of ribonucleoprotein (RNP) complex, from multiple plasmids, whose transcription was driven by the T7 promoter following the expression of T7 polymerase

(31). This system provided T7 polymerase in the cytoplasm avoiding issues with nuclear processes such as splicing and export of transcripts. To generate authentic 3' ends of the viral minigenome RNAs, some minigenome systems used a hepatitis delta virus (HDV) ribozyme at the 3' end since it has autocatalytic cleavage properties (91). Finally, without the need of a helper virus, the first infectious cDNA for a negative-strand virus was established with rabies virus in 1994 (111). In this system, the functional infectious RNP complex was reconstituted by expressing the viral nucleocapsid protein (N), polymerase cofactor protein (P), and RdRp as well as the full-length anti-genomic RNA (cRNA) from T7 promoter-driven plasmids; the exact 3' end was generated by HDV ribozyme cleavage. One of the critical steps was providing anti-genomic (positive-sense) RNA transcripts because it could minimize hybridization of N, P, and L mRNAs with genomic sense (negative-sense) RNA. Subsequently, the first infectious cDNA system for a segmented negative-strand RNA virus, Bunyamwera virus (BUNV) of the family *Bunyaviridae*, was developed using the same approach (21). Since then, reverse genetics systems for a number of non-segmented negative-strand RNA viruses have been established using basically similar approaches (31, 90).

Among the family Bunyaviridae, an infectious cDNA system has been established only for Bunyamwera virus (BUNV) (21) and La Crosse virus (LACV) (18), which belong to the genus *Orthobunyavirus*, but no system have been reported for viruses from the other four genera of the family. However, thus far, minigenome (or minireplicon) systems have been developed in BUNV (34), LACV (17), Crimean-Congo hemorrhagic fever virus (CCHFV) (41), Hantaan virus (39), Uukuniemi virus (UUKV) (42), and RVFV (82, 102).

13

**III. VIRUSES AND APOPTOSIS**

**General feature of apoptosis**

Apoptosis, programmed cell death, is one type of animal cell death accompanied by characteristic morphological change of dying cells which can be distinguish from those of accidental cell death such as necrosis and another type of cell death (65). Apoptosis also is associated with chromatin condensation, a degradation of chromosomal DNA into oligonucleosome-size fragments, membrane blebbing, cell shrinkage, and compartmentalization of the dead cells into membrane-enclosed vesicles (apoptotic bodies) (29). Another biochemical marker is a translocation of phosphatidylserine molecules from the inner leaflet to the outer leaflet of cytoplasmic membranes upon apoptotic stimuli (86). This appearance helps macrophages to recognize the dying cells and to eliminate them by phagocytosis, which prevents the leakage of toxic materials from the dead cells and subsequent induction of unregulated inflammatory reactions at the site of cell death.

Apoptosis is triggered by various kinds of stimuli including virus infection (125). The apoptotic process can be divided into two major pathways: the mitochodria-mediated intrinsic pathways and death receptor-mediated extrinsic pathway. The intrinsic pathway is triggered by an internal sensor signal such as the tumor suppressor protein p53, while the extrinsic pathway is initiated by external stimuli such as tumor necrosis factor (TNF)-family ligands. In addition to these two pathways, massive accumulation of protein molecules and abnormal folding in the ER generates significant stress (ER stress) on cells, resulting in the induction of a third form of apoptosis (37).

14

A group of caspases, which are aspartate-specific proteases and conserved among eukaryotic species, are involved in initiation, execution, and regulatory phases of these pathways (75). Thus far, fourteen caspases have been identified and some of them are critical in apoptosis (77). They are present as inactive proenzymes that are coordinately activated by dimerization or caspase-specific cleavage (19). There are at least two general classes of apoptotic caspases: upstream initiator caspases (caspases 2, 8, 9, and 10) and downstream effector caspases (caspases 3, 6, and 7). Initiator caspases are present as monomers (inactive forms) and activated by forming dimers and complexes with other regulatory proteins (e.g. FADD, TRADD etc) facilitating autocatalysis in response to apoptotic signals, while effector caspases are activated in a cascade through cleavage by initiator caspases (19). Once effector caspases are activated, they cleave a number of specific substrates leading to destruction of cell-cell interactions and nuclear structure, reorganization of the cytoskeleton, inhibition of DNA synthesis, repair and splicing, degradation of DNA, and disintegration of the entire cell contents into apoptotic bodies (75).

**Virus-induced apoptosis**

The first demonstration of virus-induced apoptosis is finding that a mutant of adenovirus lacking the expression of its E1B-19K induces severe cytopathic effect of the infected cells with a significant decrease in the yield of progeny viruses (99). Subsequently, apoptosis, as well as premature lysis of the virus-infected cells, was observed in infection with an insect virus (baculovirus) with reduction of in vitro replication and in vivo infectivity of the virus (26, 27), suggesting that the major significance of apoptosis is an abortion of virus multiplication by the premature lysis of

infected cells; a nonspecific defense mechanism against virus infection in eukaryotic cells (73). Although, since then, a number of animal viruses have been shown to induce apoptosis in infected cells and the induction of apoptosis becomes a kind of general response in the virus-infected cells, premature cell death and the subsequent abortion of the progeny virus production are not always observed in animal virus infection (72).

Even though we have little information about viral components or processes that actually trigger apoptosis, there are several different types of virus-induced apoptosis. One of them is a characteristic of cells infected with RNA viruses that express viral proteins interfering with the regulation of host macromolecule synthesis, concomitantly with virus replication. Inhibition or induction of a set of host cellular genes can alter cellular homeostasis, resulting in apoptosis through the intrinsic pathway. Eventually, double-strand RNAs (dsRNAs) are produced as an intermediate during RNA virus replication. Detection of these dsRNAs by host cellular sensors such as PKR and RIG-I can be involved in apoptosis and IFN responses of the infected cells (9, 10, 51). In addition, massive expression of viral proteins often causes misfolding or unfolding, and overloading of viral proteins in the ER, which can also induce ER stress and subsequent cell death (72, 105).

Some viruses can induce apoptosis of infected cells without their replication and de novo synthesis of proteins. For example, the infected cells can undergo apoptosis in the presence of inhibitors of protein synthesis (cycloheximide) and transcription (actinomycin D) or by infection with replication-incompetent viruses generated either by genetic mutation or treatment with ultraviolet (UV) irradiation (105). This type of apoptosis would be triggered by the binding of virion to cell surface receptors and/or the

subsequent entry of viruses. In addition, some of virion components would directly activate one of the apoptotic pathways in infected cells.

**Viral escape from apoptosis**

Apoptosis is considered as a nonspecific defense mechanism against virus infection in eukaryotic cells by limiting virus multiplication and propagation. To counter the proposed antiviral role of apoptosis, viruses have acquired various strategies to escape apoptosis of infected cells (72). One of these strategies is to overcome the limited time for viral replication, due to apoptosis, by a rapid multiplication. Indeed, many RNA viruses are known to induce apoptosis, but their proliferation is not affected by apoptosis. Vesicular stomatitis virus (VSV) induces massive apoptosis in infected cells, while the kinetics of viral growth reaches a plateau before extensive cell death (71). Similar phenomena have been observed when cells are infected with influenza virus (76) and poliovirus (73). These observations suggest that these viruses and probably many other RNA viruses are able to grow rapidly and complete virus multiplication before the onset of virus-induced apoptosis (72). Although virus-induced apoptosis cannot lead to the abortion of infection in these animal virus-infected cells directly, it should be considered that the induction of the apoptotic process can be accelerated in infected cells by inflammatory cytokines under a certain physiological condition, resulting in significant inhibition of virus proliferation (72).

Unlike RNA viruses, many DNA viruses, such as poxviruses, herpesviruses, and adenoviruses, do not induce apoptosis in productively infected cells, mainly due to the function of some viral antiapoptotic gene products capable of suppressing the apoptotic response in infected cells. Poxviruses can successfully evade the inflammatory response

and apoptosis by expressing viral proteins (CrmB and CrmC) that mimic TNF-family death receptors. These viral proteins can be secreted and bind to TNF$\alpha$/$\beta$ acting as competitive anti-inflammatory molecules as well as inhibitors of TNF-induced apoptosis (53). Both poxviruses and herpesviruses encode proteins containing high homology to the death effector domain (DED) responsible for linking death receptors and the FADD adapter protein to procaspase-8. These proteins, termed viral FLICE-inhibitory proteins (vFLIPs), bind to FADD or procaspase-8 and inhibit caspase-8 activation in response to death receptor signaling (11).

A number of viral proteins can inhibit caspase activity by either direct or indirect ways in order to prevent apoptosis. The first viral caspase inhibitor to be identified was CrmA, a product of cowpox virus, which is a homologue of mammalian serpins, a family of chymotrypsin-like serine proteinases. This protein inhibits caspase-1,-8 and -10 by acting as a pseudosubstrate of caspases. Since then, it has been reported that many poxviruses have similar gene products (23, 105). The next caspase inhibitor was found in insect viruses. P35 and the related p49 from baculoviruses can inhibit a broad range of mammalian caspases as well as insect caspases (23, 105). In addition, both baculoviruses and certain poxviruses encode functional homologues (vIAP) of cellular inhibitor of apoptosis proteins (cIAPs). The IAPs contain a conserved RING finger and one or more cys/his motifs, termed baculovirus IAP repeats (BIR), which are important for antiapoptotic activity. They appear to suppress apoptosis by binding and inhibiting the effector procaspases and caspase-9 (23, 105). Further, a variety of unique mechanisms adopted by several other viruses to inhibit apoptosis have been identified, such as the expression of Bcl-2 homologues or inhibitors of p53, inhibition of interferon responses,

18

transcriptional regulation of host proapoptotic or antiapoptotic genes, and enhancement of cell survival signals (9, 72, 105).

# Chapter 2:  Rescue of Infectious Rift Valley Fever Virus Entirely from cDNA

## I. INTRODUCTION

RVFV causes an endemic disease of sub-Saharan Africa that has emerged in explosive mosquito-borne epidemics resulting in massive economic loss in herds of sheep and cattle. This virus also causes hemorrhagic fever, encephalitis, retinal vasculitis, and lesser disease in humans.  In addition to the epidemics in sub-Saharan Africa, RVFV has been exported to Egypt on multiple occasions, particularly in 1977 when thousands of human infections occurred (97).  After a particularly large epidemic in Africa in 1997-8, the virus traveled to Egypt and the Arabian peninsula, menacing further spread (113, 134).  The possibilities of introduction in many different countries and of its use as a bioterrorist agent (92) demand the availability of effective protective measures for humans and domestic animals.

It is likely that the disease can only be controlled by an effective live attenuated vaccine for livestock, and certainly the control activities will necessitate protection of humans, most likely by vaccination (93).  Available livestock vaccines are unsatisfactory either because of fetal pathology or lack of immunogenicity; and modern usage requires the presence of markers to identify vaccinated animals in contrast to those after natural infection.  The basis of attenuation of the single viable human vaccine candidate is unknown (24, 131), which hampers further development.  A lack of understanding of the molecular virology of *Bunyaviridae* and of its medically important genus *Phlebovirus* is a major barrier to further vaccine development.  The ability to recover RVFV from DNA constructs would permit rapid progress in all these areas.

20

Reverse genetics has been established for several RNA virus families, but *Arenaviridae* and *Bunyaviridae* have been recalcitrant. Among the family *Bunyaviridae,* only Bunyamwera virus (BUN) (21) and La Crosse virus (LAC) (18) belonging to the genus *Orthobunyavirus* have been successfully recovered from cDNA. No viruses from the other four *Bunyaviridae* genera have been recovered. The *Phlebovirus* genus, in particular, has a number of important human and animal pathogens, is poorly understood at the molecular level, and has a replication strategy that, unlike other *Bunyaviridae* but resembling arenaviruses, utilizes an ambisense coding strategy (109). This chapter will demonstrate the development of a reverse genetics system for RVFV, which can in particular advance our knowledge of its molecular virology.

## II. MATERIALS AND METHODS

### Media, cells and viruses

Vero, Vero E6, 293 (human embryonic kidney) and MRC5 (human diploid fibroblast) cells were maintained in Dulbecco's modified minimum essential medium (DMEM) containing 10% fetal bovine serum (FBS). BHK-21 cells and BHK/T7-9 cells which express T7 RNA polymerase (58) were grown in MEM-alpha containing 10% FBS. Penicillin (100 U/ml) and streptomycin (100 µg/ml) were added to the media. BHK/T7-9 cells were selected in medium containing 600 µg/ml hygromycin. RVFV vaccine strain MP-12 was grown in BHK-21 cells, and infectivity was assayed by plaques in Vero E6 cells.

**Plasmid construction**

RVFV viral RNAs were extracted from lysates of Vero E6 cells infected with the MP-12 strain and were used for first-strand cDNA synthesis with random hexamer primers using Ready-To-Go You-Prime First-Strand beads (Amersham Biosciences) according to the manufacturer's instructions. The first-strand cDNA was used for amplification of segments and genes of interest to construct plasmids. MP-12 strain full-length S, M, and L segments were cloned between *Kpn* I and *Not* I sites of the pPro-T7 plasmid which originated from pSinRep5 (Invitrogen) to express full length anti-viral-sense segments, resulting in pPro-T7-S(+), pPro-T7-M(+) and pPro-T7-L(+). An *Xho*I site was introduced into each of S, M and L sequences by site-directed mutagenesis (Fig. 2.1A). The pPro-T7-S(-), pPro-T7-M(-) and pPro-T7-L(-) were constructed using a similar strategy. The pT7-IRES-vN, pT7-IRES-vNSs and pT7-IRES-vL expressing N, NSs and L protein of MP-12 strain, respectively, were constructed by PCR amplification of ORFs of N, NSs, and L, and cloning into a modified pBL-EMCV (pBluscript plasmid origin), pT7-IRES. The pCAGGS-vG, which expresses 78-kDa, NSm, G2, and G1 proteins, was made by introducing an *Eco*RI site upstream of the first ATG codon of the ORF in pPro-T7-M(+), and an *Xho*I site introduced downstream of the stop codon. The *Eco*RI-*Xho*I fragment was cloned into the multicloning site of pCAGGS plasmid (Illustration 2.1).

**Virus rescue**

Subconfluent monolayers of BHK/T7-9 cells in 60 mm dishes were co-transfected with pPro-T7-S(+), pPro-T7-M(+), pPro-T7-L(+), pT7-IRES-vN and pCAGGS-vG, all of which were 2.2 μg, and 1.1 μg of pT7-IRES-vL using TransIT-LT1 (Mirus). Twenty-

four hrs later, culture medium was replaced with fresh medium. Five days later, the culture supernatants were passaged into BHK-21 cells.

**RT-PCR analysis**

Viral RNA was extracted from culture supernatants of Vero E6 cells infected with MP-12 or the recovered MP-12 (rMP-12) by High pure Viral RNA kit (Roche Applied Science). After DNase I digestion of the samples at 37°C for 1 hr, RT-PCR was performed with and without reverse transcription using Ready-To-Go RT-PCR Beads (Amersham). Primer pairs to amplify segments were S898F/S1480R, M2681F/M3300R, and L3603F/L4245R, respectively. The numbering refers to the segment, position and orientation of the primers on the RVFV antiviral-sense genomes.

**Plaque assay**

After virus adsorption to Vero E6 cells at 37°C for 1 hr, inocula were removed, and cells were overlaid with DMEM containing 0.9% agar and 5% FCS. After 2 days incubation, cells were stained with neutral red for 16 hours. Alternatively, I used minimum essential medium containing 0.6% tragacanth gum (MP Biomedicals, inc.), 2.5% FCS, and 5% tryptose phosphate broth for the overlay. After 3 days, the overlay was removed, fixed and stained with 0.75% crystal violet, 10% formaldehyde, and 5% ethanol.

**Northern blot analysis**

RNA was extracted from purified viruses using TRIzol Reagent. Approximately 100 ng of RNA was denatured and separated on 1 % denaturing agarose-formaldehyde gels and transferred onto a nylon membrane (Roche Applied Science). Northern blot analysis was performed with viral-sense S-, M-, and L-specific RNA probes. Hybridization was performed at 68 °C for 18 h in standard hybridization buffer with 50 % formamide, and subsequent washing of the membrane with 2×SSC at room temperature and 0.5×SSC at 55 °C (1×SSC is 0.15 M NaCl plus 0.015 M sodium citrate).

**Analysis of viral growth**

Vero E6 cells, 293 cells, and MRC5 cells were infected with viruses at an moi of 1 or of 0.01 at 37˚C for 1 hr, washed 3 times with PBS, and medium added. Culture supernatants were harvested at indicated hours postinfection (p.i.) in Fig. 2.3., and the virus titer measured by plaque assay. The growth curves were shown as mean +/- standard deviation from three independent experiments.

**III. RESULTS**

**Recovery of RVFV from cDNAs**

To recover MP-12 from cDNAs, several plasmids, encoding RVFV MP-12 proteins and viral RNAs, were constructed. The entire region of each viral RNA segment was placed between a T7 promoter and a hepatitis delta virus ribozyme in each RNA

## A. Genome RNA expression plasmids

pProT7-vS(+)

pProT7-vM(+)

pProT7-vL(+)

## B. Viral protein expression plasmids

pT7-IRES-vN

pT7-IRES-vNSs

pCAGGS-vM

pT7-IRES-vL
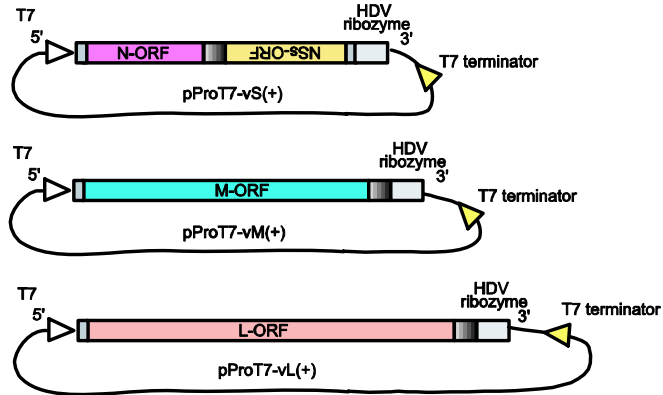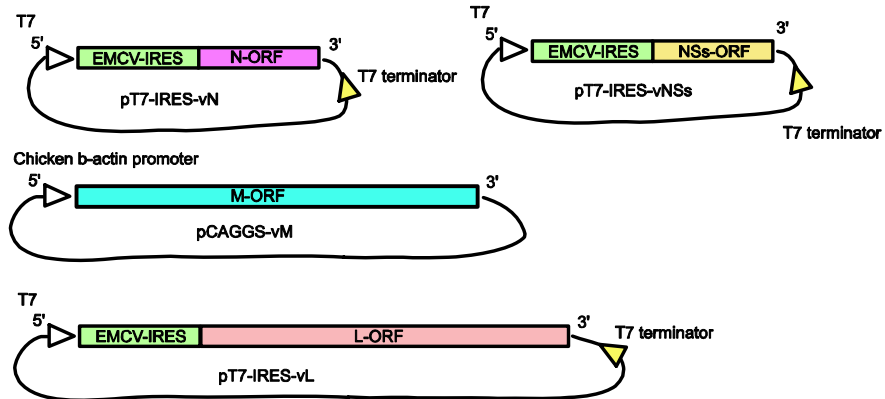
Illustration 2.1: Schematic diagram of plasmid constructs for genomic RNA expression (A) and viral protein expression (B)

expression plasmid.  The entire N, L and NSs gene ORFs were placed independently downstream of a T7 promoter and an encephalomyocarditis virus (EMCV) internal ribosome entry site (IRES) in each protein expression plasmid, while the entire M gene ORF was cloned in a eukaryotic expression vector, pCAGGS (Illustration 2.1). To recover infectious viruses, BHK/T7-9 cells, which stably express high levels of T7 RNA polymerase under the chicken-beta-actin promoter control (58), were cotransfected with various combinations of these plasmids (Table 2.1).  Five days after transfection, the supernatants were transferred into Vero E6 or BHK-21 cells to amplify released viruses. In five repeated experiments, infectious viruses were recovered from BHK/T7-9 cells that were transfected with plasmids expressing all three antiviral-sense RNA fragments and plasmids expressing all structural proteins (Tables 2.1 and 2.2).  Low titers of progeny were detected 3 days post transfection and steadily increased until 5 days (Table 2.2). The recovery of RVFV was unsuccessful when the plasmid expressing NSs protein (pT7-IRES-vNSs) was included (Table 2.1).  In some experiments viruses were recovered without the plasmid expressing envelope proteins (pCAGGS-vG) and even in the absence of all structural protein expression plasmids, demonstrating that viral structural protein expression directly from added plasmids was not an absolute requirement for virus recovery.  No virus recovery occurred after transfection of plasmids expressing viral-sense RNA segments, yet addition of plasmids expressing L, N and envelope proteins resulted in virus recovery in two out of three experiments.

To exclude the possibility that recovered viruses represented contamination with MP-12, I modified all three RNA expression plasmids to carry a unique *Xho*I site, which introduced a silent mutation in the NSs, Gc and L genes (Fig. 2.1A).  The modified RNA expression plasmids were cotransfected with plasmids, each expressing L, N and

envelope proteins into BHK/T7-9 cells. RT-PCR amplification of the recovered viral RNA and subsequent digestion of the PCR products with *Xho*I showed that the recovered viruses (rMP-12) carried the introduced *Xho*I site in each RNA segment (Fig. 2.1B). After over 10 passages of virus in Vero E6, sequence analysis was performed and showed that the rescued rMP-12 retained the introduced *Xho*I sites of all three segments, while other sequences were exactly corresponded to those of the parental MP-12. These data unambiguously established the validity of this reverse genetics system.

**Analysis of plaque morphology in infected cells and viral RNAs of virions**

To examine whether the rescued rMP-12 form plaques with morphology comparable to that of the parental MP-12, plaque assay was performed with two different methods as described in the Material and Methods. In both methods, similar sizes of clear plaques were observed of approximately 1 mm in diameter in both MP-12 and rMP-12-infected Vero E6 cells (Fig. 2.2A). I also observed that the majority of cells were detached at 2 to 3 days after infection with rMP-12, similar to MP-12 infection.

Next I analyzed and compared viral RNA in purified MP-12 and rMP-12 by Northern blot analysis. To purify viruses, MP-12 and rMP-12 were propagated in Vero E6 cells after inoculation at a multiplicity of infection (MOI) of 0.1. At 48 h p.i., culture fluids were collected and clarified by low-speed centrifugation. Then virus particles were partially purified by two subsequent ultracentrifugation steps using a discontinuous sucrose gradient consisting of 60, 50, 30, and 20% sucrose (56). The virus particles at the interface of 30 and 50% sucrose were collected, diluted, and then further applied on a continuous sucrose gradient of 20 to 60% sucrose at 28,000 rpm for 18 h using a Beckman SW28 rotor. I could obtain the majority of virus particles in fraction 7 (1.16

27

Table 2.1: Plasmid combination for the rescue of RVFV

| Plasmid (µg/60mm dishes) or parameter | Plasmid combination or value | | | | | |
|---|---|---|---|---|---|---|
| | A | B | C | D | E | F |
| pPro-T7-S(+) (2.2) | + | + | + | + | - | - |
| pPro-T7-M(+) (2.2) | + | + | + | + | - | - |
| pPro-T7-L(+) (2.2) | + | + | + | + | - | - |
| pPro-T7-S(-) (2.2) | - | - | - | - | + | + |
| pPro-T7-M(-) (2.2) | - | - | - | - | + | + |
| pPro-T7-L(-) (2.2) | - | - | - | - | + | + |
| pT7-IRES-vN (2.2) | + | + | + | - | + | - |
| pT7-IRES-vL (1.1) | + | + | + | - | + | - |
| pCAGGS-vG (2.2) | + | + | - | - | + | - |
| pT7-IRES-vNSs (2.2) | - | + | - | - | - | - |
| Virus rescue* | 3/3 | 0/3 | 2/3 | 1/3 | 2/3 | 0/3 |
| Titer (PFU/ml) | | | | | | |
| Exp. 1 | $1.0 \times 10^5$ | 0 | $3.0 \times 10^4$ | $4.8 \times 10^5$ | $2.3 \times 10^3$ | 0 |
| Exp. 2 | $5.0 \times 10^4$ | 0 | $1.3 \times 10^6$ | 0 | $3.7 \times 10$ | 0 |
| Exp. 3 | $3.0 \times 10^4$ | 0 | 0 | 0 | 0 | 0 |

*Efficiency of rescue in 3 experiments.


Table 2.2: Time course of recombinant RVFV production*

| Hours after infection | 24 | 48 | 72 | 96 | 120 |
|---|---|---|---|---|---|
| Titer (PFU/ml) | | | | | |
| Exp. 4 | 0 | 0 | $2.8 \times 10^2$ | $4.5 \times 10^3$ | $5.3 \times 10^6$ |
| Exp. 5 | 0 | 0 | $2.0 \times 10$ | $1.0 \times 10^3$ | $8.5 \times 10^5$ |

*Plasmid combination A in Table 2.1 was used for this study.

**A**

```
                          419
                     silent mutation
            5'                          3'
MP-12 Sv    CTAAGCTCTACTAGAGTGCATAGG
rMP-12 Sv   CTAAGCTCTACTCGAGTGCATAGG
                        XhoI
aa. (NSs)    L   S   S   T   R   V   H   R
```

```
                     3478 3480
                    silent mutation
            5'                          3'
MP-12 Mvc   ATAGATCAATTGGAGTGCACAACA
rMP-12 Mvc  ATAGATCAACTCGAGTGCACAACA
                        XhoI
aa. (G1)     I   D   Q   L   E   C   T   T
```

```
                     3814 3816
                    silent mutation
            5'                          3'
MP-12 Lvc   GAGCTATTCTTAGAGTATAAGAAG
rMP-12 Lvc  GAGCTATTCCTCGAGTATAAGAAG
                        XhoI
aa. (L)      E   L   F   L   E   Y   K   K
```

**B**

Figure 2.1: Introduction of gene marker into S, M, and L segments

(A) Alignment of nucleotide and amino acid (aa.) sequences. Introduced *Xho*I sites and mutation positions on each segment were underlined and shown as arrowhead, respectively. (B) Demonstration of the *Xho*I marker in rMP-12 RNA. Viral RNA was extracted from culture supernatants of Vero E6 cells infected with MP-12 and rMP-12 and was treated with DNase I at 37°C for 1 h, PCR was performed with (+) and without (−) the reverse transcription step (RT). Digestion with *Xho*I was performed at 37°C for 2 h. The expected sizes of digested fragments are shown to the right of the gels.

29

g/cm$^3$ in density) among 10 fractions as described in the previous study (56). The virus particles in fraction 7 were concentrated through a 20% sucrose cushion at 38,000 rpm for 2 h using a Beckman SW41 rotor and subjected to RNA extraction. Riboprobes, pN-S(-), pM(-), and pL(-), were used for the detection of viral-sense S, M, and L segments of viruses, respectively; pN-S(-), pM(-), and pL(-) are complementary to nt 915 to 1652 from the 5' end of viral-sense S, nt 1784 to 2589 from the 5' end of viral-snese M, and nt 5649 to 6386 from the 5' end of viral-sense L, respectively. Northern blot analysis of the sucrose gradient-purified viruses showed that the rescued rMP-12 successfully contained comparable levels of all three segments to those of MP-12 (Fig. 2.2B).
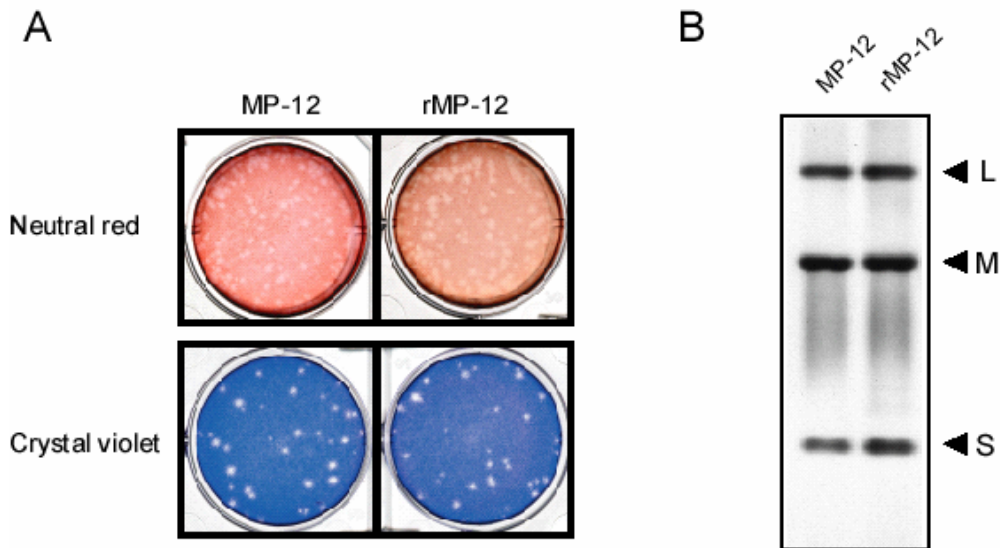


Figure 2.2: Comparison of plaque morphology and viral RNAs of MP-12 and rMP-12

(A) Plaque production in Vero E6 cells by MP-12 and rMP-12 stained with neutral red and crystal violet. (B) Purified virion RNAs of MP-12 and rMP-12 were analyzed by Northern blotting using virus-sense S-, M-, and L-specific RNA probes.

**Analysis of growth kinetics of recovered viruses in Vero cells, 293 cells, and MRC5 cells**

Analysis of one-step growth kinetics of MP-12 and the recovered rMP-12 in Vero cells lacking interferon (IFN) alpha/beta genes (32, 89) and 293 cells showed that the kinetics of infectious rMP-12 were similar to those of MP-12 in both cells (Fig. 2.3A and B). In addition, after infection of these viruses in MRC5 cells, which are human lung diploid fibroblast cells and strongly interferon-competent cells, at a low MOI of 0.01 as well as an MOI of 0.1, both MP-12 and rMP-12 replicated efficiently (Fig. 2.3C and D).

**A.** Vero cells (MOI: 1.0)
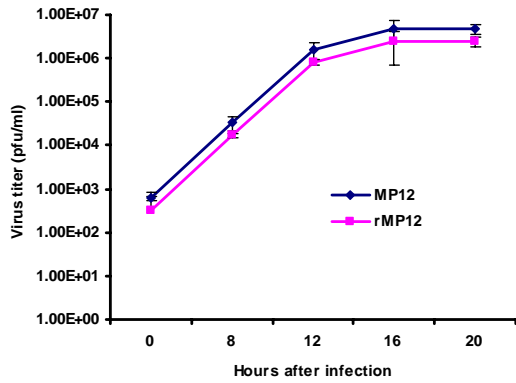


**B.** 293 cells (MOI: 1.0)
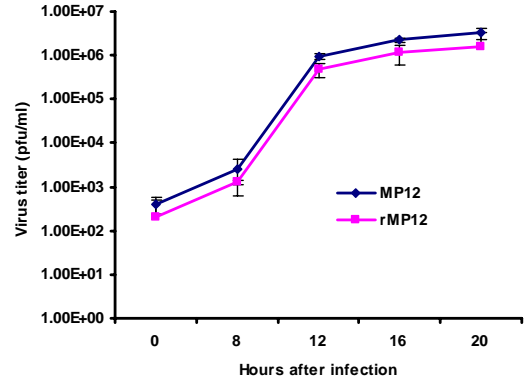


**C.** MRC5 cells (MOI: 1.0)
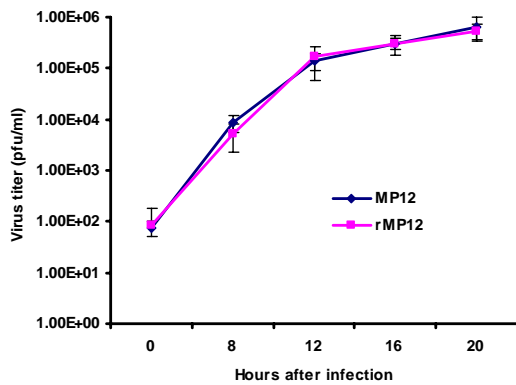


**D.** MRC5 cells (MOI: 0.01)
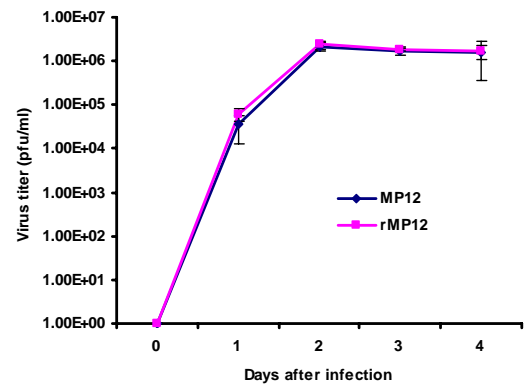


Figure 2.3: Growth curves of MP-12 and rMP-12

Vero cells (A), 293 cells (B), and MRC5 cells (C and D) were infected with MP-12 and rMP-12 at an MOI of 1 (A, B, and C) or 0.01 (D), and the culture supernatants were collected at the indicated time points. Culture supernatants were collected from three independent wells at each time point, and the virus titers were determined in Vero E6 cells by plaque assay. The values are mean titers with standard deviations.

# Chapter 3: NSm and 78-Kilodalton Protein of Rift Valley Fever Virus are Nonessential for Viral Replication in Cell Culture

## I. INTRODUCTION

Rift Valley fever virus (RVFV) (of the genus *Phlebovirus*, family *Bunyaviridae*), which is the cause of severe epidemics among ruminants of sub-Saharan Africa, is also recognized as a human pathogen that can cause a syndrome with fever and myalgia, a hemorrhagic syndrome, ocular disease, and encephalitis (7, 94, 97). RVFV has a single-stranded, tripartite RNA genome composed of the L, M, and S segments. The L segment encodes the L protein, an RNA-dependent RNA polymerase. Using an ambisense strategy, the S segment expresses the N protein and the nonstructural protein NSs (108).

The RVFV M segment encodes four proteins, two major envelope glycoproteins, Gn (or G2) and Gc (or G1) that most probably bind to an as-yet-unknown viral receptor molecule(s) to initiate virus infection, and two minor proteins, the 14-kDa nonstructural NSm protein (61) and the 78-kDa protein, which is reported to be a structural protein (121). The biological functions of NSm and the 78-kDa protein are totally unknown, but they probably do not have a role in viral RNA synthesis; RVFV minigenome RNA replication and transcription occur efficiently in the absence of expression of the NSm, 78 kDa, Gn and Gc proteins (54). The region upstream from the Gn gene (pre-Gn region) contains five in-frame AUG codons (Illustration 3.1), and it appears that each of these five AUGs serves as an initiation codon of different proteins; the first AUG, the second AUG and the third-to-fifth AUGs serve as an initiation codon(s) to generate the 78-kDa protein, NSm, and the Gn-Gc fusion protein, respectively (61, 110, 124). The 78-kDa

protein consists of pre-Gn region and Gn regions.  NSm contains the region that starts from the second AUG to the end of the pre-Gn region.  A precursor of the Gn/Gc fusion protein is translated from the third-to-fifth AUG, and then it undergoes protein processing to generate Gn and Gc proteins.  Gn and Gc protein synthesis still occurs in the absence of the first and second AUGs (62, 124).

In the study presented in this chapter, using a reverse genetics system of the MP-12 strain as described in chapter 2, I have successfully recovered several recombinant RVFV mutants carrying mutations in the pre-Gn region of the M segment, one lacking NSm protein expression, one lacking 78-kDa protein expression, and one lacking expression of both proteins. All of the mutants and their parental virus produced plaques with similar sizes and morphologies in Vero E6 cells and had similar growth kinetics in Vero, C6/36, and MRC5 cells, demonstrating that the NSm and 78-kDa proteins were not needed for the virus to replicate efficiently in cell culture. A competition-propagation assay revealed that the parental virus was slightly more fit than the mutant virus lacking expression of both proteins.

## II. MATERIALS AND METHODS

### Media, cells and viruses

Vero, Vero E6 and MRC5 (human lung diploid fibroblast) cells were maintained in Dulbecco's modified minimum essential medium (DMEM) containing 10% fetal calf serum (FCS).  C6/36 (Mosquito larvae, *Aedes albopictus*) cells were maintained in Leibovitz L-15 medium complemented with 10% FCS at 28°C. BHK/T7-9 cells which

express T7 RNA polymerase were grown in MEM-alpha containing 10% FCS.  Penicillin (100 U/ml) and streptomycin (100 μg/ml) were added to the media.  BHK/T7-9 cells were selected in medium containing 600 μg/ml hygromycin.

**Plasmids**

pPro-T7-avS(+), pPro-T7-avM(+) and pPro-T7-avL(+), which express full length antiviral-sense RNAs without gene markers (*Xho*I sites) on each segment described in Chapter 2, were used for virus rescue.  pT7-IRES-vN, pT7-IRES-vL, and pCAGGS-vG expressing N, L, and all M segment proteins (78kDa, NSm, Gn, and Gc), respectively, were also used.  To make mutant constructs lacking expression of  the NSm and/or the 78-kDa proteins, mutations were introduced into the second and/or first translation initiation codons  (AUGs) of the pre-Gn region of pPro-T7-avL (+) by site-directed mutagenesis using QuickChange site-Directed Mutagenesis kit (Stratagene), resulting in pPro-T7-avM(+)-delNSm-1,  pPro-T7-avM(+)-delNSm-2,  pPro-T7-avM(+)-del78,  and  pPro-T7-avM(+)-delNSm/78 (Illustration 3.1).

**Antibodies**

Rabbit anti-NSm antibody was prepared by inoculating rabbits with purified recombinant glutathione S-transferase (GST)-NSm fusion protein (amino acids 60 to 115 of NSm protein were fused with the C-terminus of GST protein) expressed in *E. coli*, and the sera were subsequently affinity-purified with the GST-NSm fusion protein.  Anti-N rabbit polyclonal antibody was also prepared by injecting a rabbit with GST-N fusion protein (the entire N protein was fused with the C-terminus of GST protein) followed by affinity purification of the serum by the GST-N fusion protein. A mouse polyclonal antibody

against RVFV was obtained from Dr. R. B. Tesh (UTMB). Monoclonal antibodies against Gn (R1-4D4) and Gc (R1-5G2) were obtained from Dr. George Ludwig, (USAMRIID, Ft. Detrick, Frederick, MD).

**Rescue of mutant viruses**

As described in the Chapter 2, BHK/T7-9 cells were grown in 60-mm dishes and transfected with mixtures of plasmids including 2.5 μg each of pPro-T7-avS(+), pPro-T7-avM(+), pPro-T7-avL(+), pT7-IRES-vN, pCAGGS-vG, and 1.25 μg of pT7-IRES-vL using TransIT-LT1 (Mirus). To rescue mutant viruses, pPro-T7-avM(+) was substituted with pPro-T7-avM(+)-delNSm-1, pPro-T7-avM(+)-delNSm-2, pPro-T7-avM(+)-del78, or pPro-T7-avM(+)-delNSm/78. Twenty-four hours later, the culture medium was replaced with fresh medium. Five days later, the culture supernatants were collected and stored at -80 °C for amplification and further characterization of mutant viruses.

**Plaque assay**

After virus adsorption to VeroE6 cells at 37°C for 1 hr, the inocula were removed, and cells were washed three times with PBS to remove unattached viruses. The cells were overlaid with minimum essential medium (MEM) containing 0.6 % tragacanth gum (MP Biomedicals, inc.), 2.5 % FCS, and 5 % tryptose phosphate broth (TPB). At 3 days post-infection (p.i.), the overlay was removed, and cells were fixed and stained with 0.75 % crystal violet, 10 % formaldehyde, and 5 % ethanol.

**Western blot analysis**

Western blot analysis was performed as described previously (56). Infected cells were lysed with a sample buffer and subjected to sodium dodecyl sulfate-polyacrylamide gel electrophoresis (SDS-PAGE). The separated proteins were transferred to polyvinylidene difluoride (PVDF; BioRad) membrane. After blocking for 1hr, the membranes were incubated with primary antibody overnight at 4°C and with secondary antibody for 1 hr at room temperature. The membrane was developed with an enhanced chemiluminescence (ECL) kit (Amersham Biosciences).

**Analysis of viral growth**

Vero cells, MRC5 cells, and C3/36 cells were independently infected with mutant viruses or parental virus arMP-12 at an MOI of 1 or 0.01. After 1 hr adsorption, the inocula were removed, and cells were washed 3 times with PBS. Culture supernatants were harvested at the indicated time points, and the virus amounts were titrated by plaque assay on Vero E6 cells.

**Radioimmunoprecipitation (RIP)**

Vero E6 cells were infected with viruses at an MOI of 1. At 8 h p.i., cells were incubated in methionine free medium for 30 min, and then were labeled with 100 μCi/ml of Tran$^{35}$S-label (MP Biomedical, Inc., Irvine, CA ) for 30 min. Cell lysates were prepared with lysis buffer (1% Triton X-100, 0.5% sodium deoxycholate, 0.1% SDS in phosphate-buffered saline), and the intracellular RVFV-specific proteins were immunoprecipitated with indicated antibodies. The immunoprecipitated proteins were analyzed by 10% SDS-PAGE.

37

## III. RESULTS

### Generation of RVFV mutants lacking expression of the NSm and/or 78-kDa proteins

To determine whether the NSm and 78-kDa proteins are required for RVFV replication, I attempted to generate mutant viruses lacking the expression of one or both proteins by using a reverse-genetics system of an attenuated vaccine candidate of RVFV, MP-12. In Chapter 2, I demonstrated that MP-12 recovered by using a reverse-genetics system carries an *Xho*I site in each RNA segment, yet the rescued parental virus, arMP-12, and its mutants in this chapter did not have this restriction site in any of the three RNA segments. Of note, the recovered arMP-12 and my working stock of MP-12 virus shared identical molecular sequences in all 3 RNA segments.

To abolish expression of the 78-kDa protein, an *EcoR*I site was created at the first AUG in the pre-Gn region that altered that AUG to AUU in pPro-T7-avM(+), which expressed the anti-viral sense MP-12 M segment RNA (Illustration 3.1). The second AUG in the pre-Gn region was changed to GUG (valine) or GCC (alanine) in pPro-T7-avM(+) to abolish NSm expression. To abolish expression of both proteins, I constructed another mutant of pPro-T7-avM(+) with AUU and GCC in place of the first and second AUGs, respectively. Cotransfecting each of these pPro-T7-avM(+)-derived mutant plasmids with a mixture of plasmids expressing the S and L segment RNAs plus three viral protein expression plasmids into BHK/T7-9 cells stably expressing T7 polymerase (58) allowed us to rescue the mutant viruses. The parental pPro-T7-avM(+) was used as a positive control. At five days posttransfection, the supernatants were transferred into Vero E6 cells to amplify the rescued viruses. The induction of cytopathic effects suggested that infectious viruses were successfully recovered from all the transfected

38

samples. Viruses were recovered from pPro-T7-avM(+) bearing the GUG mutation in the second AUG (arMP-12-delNSm-1), from pPro-T7-avM(+) with the GCC mutation in the second AUG (arMP-12-delNSm-2), from pPro-T7-avM(+) with the AUU mutation in the first AUG (arMP-12-del78), and from pPro-T7-avM(+) carrying the AUU and GCC mutations in the first 2 AUGs (arMP-12-delNSm/78), as well as the parental arMP-12 (see Illustration 3.1). All of the mutant- and the parent-produced plaques were similar in size and morphology in VeroE6 cells (Fig. 3.1). Sequence analysis demonstrated that the recovered viruses carried the introduced mutation(s) and lacked other mutations in the M segment RNA.

To study the stabilities of the introduced mutations, each mutant virus was passed 11 times in Vero E6 cells. For each virus passage, cells were infected with viruses at an MOI of 0.01, and culture fluid was collected at 48 h p.i. Sequence analysis of the M segment-coding region showed that all of the mutants retained the introduced mutation. Also, infection by the viruses obtained after 11 passages resulted in the expected accumulation of intracellular NSm and 78-kDa proteins (data not shown), confirming that all mutant viruses retained the original mutations.

**Comparison of the expression of NSm, 78-kDa, Gn, and Gc proteins in infected cells with arMP-12 and mutant viruses**

I next investigated the expression of 78-kDa and NSm proteins in the cells infected with the rescued viruses. VeroE6 cells were mock-infected or independently infected with the rescued viruses at an MOI of 1. At 24 h p.i., cell extracts were prepared, and expression of NSm and the 78-kDa proteins was examined using Western
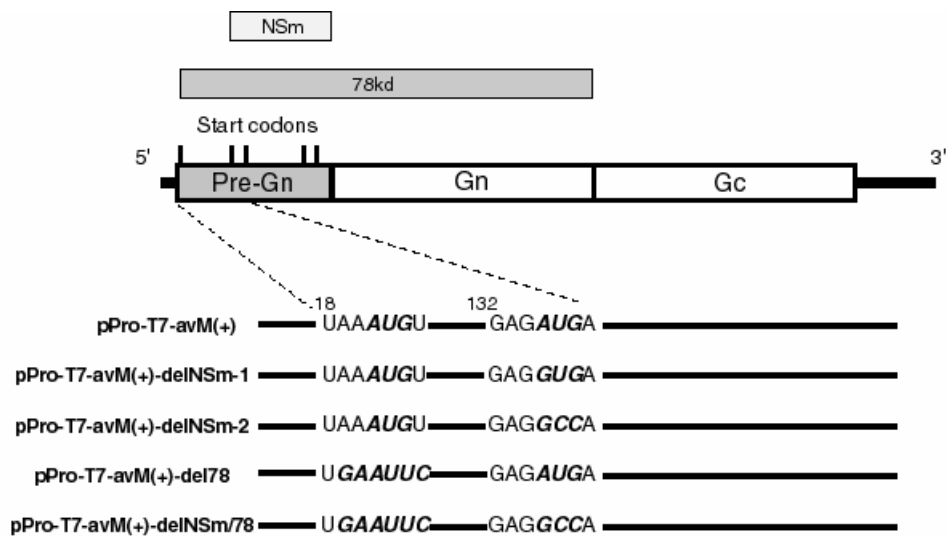
Illustration 3.1: Schematic representation of the MP-12 antiviral-sense M segment and sequences of the pre-Gn region sections

Five in-frame translation start codons in the pre-Gn region are illustrated by five short vertical lines. Regions that encode the NSm and 78-kDa proteins are represented by two boxes at the top of the diagram. The sequences around the first and second AUGs in the pre-Gn are shown at the bottom.
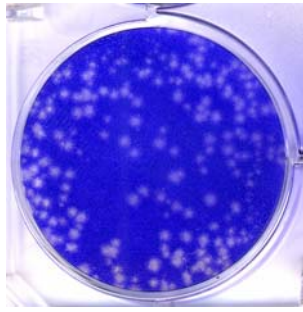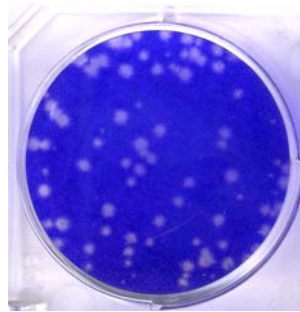
arMP-12                arMP-12-delNSm-1                arMP-12-delNSm-2
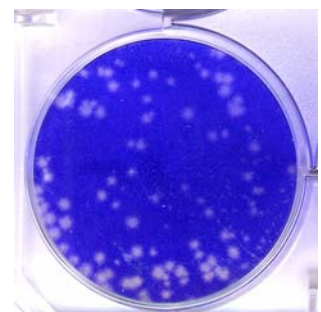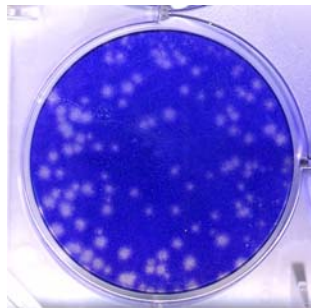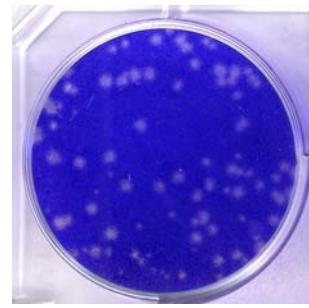
arMP-12-del78                arMP-12-delNSm/78

Figure 3.1: Plaque phenotype of mutant viruses

Vero E6 cells were independently infected with arMP-12 and its mutant viruses as indicated. Plaques were stained with crystal violet at 3 day p.i.

blot analysis with anti-NSm antibody (Fig. 3.2). Results were consistent with my expectations: the 78-kDa protein and the NSm protein were detected in the parental arMP-12-infected cells; only the 78-kDa protein appeared in the arMP-12-delNSm-1-infected cells and arMP-12-delNSm-2-infected cells, NSm was made in arMP-12-del78-infected cells, and neither protein was present in arMP-12-delNSm/78-infected cells. These data established that the first AUG and the second AUG in the pre-Gn region were indeed used for 78-kDa protein synthesis and NSm protein synthesis, respectively, in RVFV-infected cells. I noted the presence of a band(s) for 73- to75- kDa-sized protein which migrated slightly faster than the 78-kDa protein in those cells infected with arMP-12 and its mutants (Fig. 3.2, asterisk), whereas this band was not detected in mock-infected cells. The 73- to 75-kDa protein(s) was(were) dispensable for RVFV replication, because the MP-12 mutant carrying a deletion that included the first, second and third AUGs in the pre-Gn region was viable and did not produce the 73- to 75-kDa protein(s), the NSm, and 78-kDa proteins in infected cells, which will be described in Chapter 4.

Since all mutations were introduced in upstream of the Gn and Gc protein genes (pre-Gn region), the effect of the mutations on the synthesis of Gn and Gc proteins was examined (Fig. 3.3A). Vero E6 cells were mock-infected or independently infected with MP-12 and the rescued viruses at an MOI of 1. At 8 h p.i., cells were radiolabeled with 100 μCi/ml of Tran$^{35}$S-label for 30 min. Cell lysates were prepared with lysis buffer, and the intracellular RVFV-specific proteins were immunoprecipitated with anti-Gn (R1-4D4) monoclonal antibody, anti-Gc (R1-5G2) monoclonal antibody, anti-RVFV antibody (56) or anti-N rabbit polyclonal antibody. The synthesis of N protein and the mixture of Gn and Gc proteins, both of which co-migrated in the gel, were similar among the cells

that were infected with arMP-12 and all of the mutant viruses (Fig. 3.3A). Anti-Gn monoclonal antibody efficiently immunoprecipitated the 78-kDa protein, which migrated more slowly than did the Gn protein, from the extracts of the MP-12-infected cells (Fig. 3.3A, dots); however, anti-RVFV antibody did not precipitate this protein efficiently. Western blot analysis using anti-Gn monoclonal antibody and anti-Gc monoclonal antibody clearly demonstrated that arMP-12 and its mutant viruses accumulated similar amounts of Gn and Gc proteins in infected cells (Fig. 3.3B).
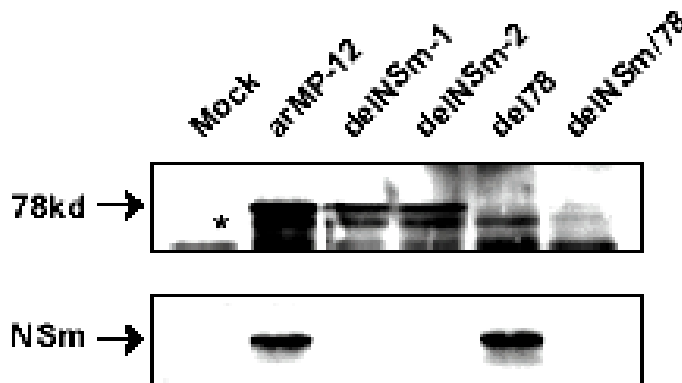


Figure 3.2: Expression of the NSm and 78-kDa proteins in infected cells with mutants

Vero E6 cells were mock-infected (Mock) or independently infected with the indicated viruses at an MOI of 1, and cell extracts were prepared using lysis buffer at 24 h p.i. Viral proteins were separated by 12 % SDS PAGE. Western blot analysis was performed using anit-NSm antibody to demonstrate the NSm and 78-kDa proteins. The asterisk represents a protein of unknown origin, which was recognized by anti-NSm antibody.
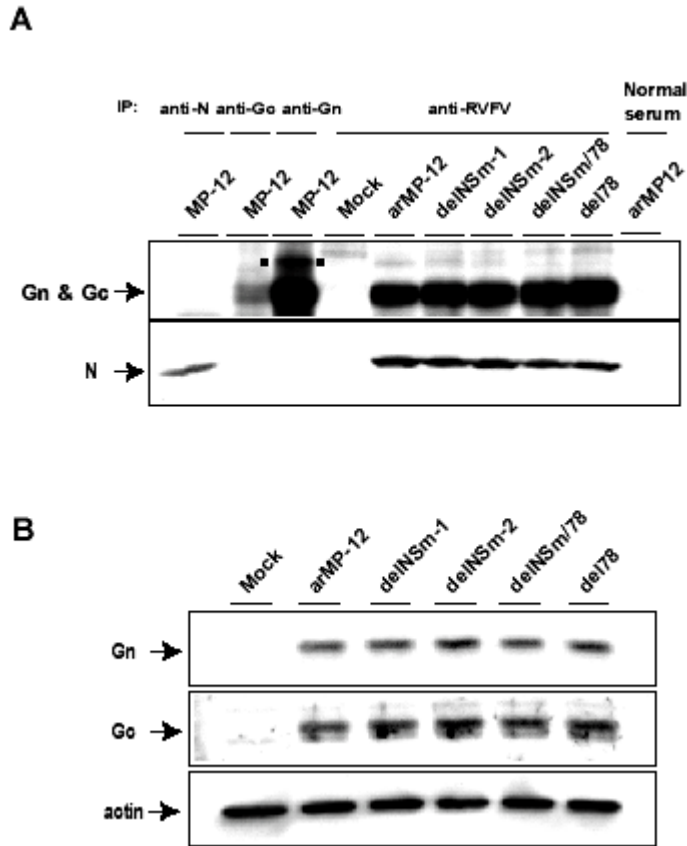
Figure 3.3: Expression of Gn and Gc proteins in infected cells with mutant viruses

(A) Vero E6 cells were mock-infected (Mock) or infected with the indicated viruses at an MOI of 1, and the cells were labeled with 100 μCi/ml of Trans$^{35}$S-label for 30 min at 8 h p.i. MP-12-specific N, Gn, and Gc proteins were immunoprecipitated using anti-N polyclonal antibody (anti-N), anti-Gn monoclonal antibody (anti-Gn), and anti-Gc monoclonal antibody (anti-Gc), respectively. Anti-Gn antibody also precipitated the 78-kDa protein (square dots). Anti-RVFV antibody was used to immunoprecipitate Gn, Gc, and N proteins of arMP-12 and its mutant viruses. Normal mouse serum (Normal serum) was used as a control. Precipitated proteins were analyzed by 10 % SDS PAGE. (B) Vero E6 cells were mock-infected (Mock) or independently infected with indicated viruses at an MOI of 1, and cell extracts were prepared at 8 h p.i. Western blot analysis was performed using anti-Gn monoclonal antibody, anti-Gc monoclonal antibody, and anti-actin antibody to detect Gn protein, Gc protein, and actin, respectively.

**Analysis of growth kinetics of mutant viruses in Vero cells, C6/36 cells, and MRC5 cells**

To evaluate the roles of the NSm and the 78-kDa proteins in RVFV replication and infectivity, one-step virus growth kinetics of the mutant viruses were analyzed in three different cell lines; interferon-incompetent Vero cells (Fig. 3.4A), *Aedes albopictus* mosquito C6/36 cells (Fig. 3.4B), and interferon-competent human lung fibroblast MRC5 cells (Fig. 3.4C). The results revealed that all of the viruses released infectious viruses into the culture fluid with similar kinetics after infection at an MOI of 1; a low titer at 8 h p.i. of arMP-12-del78 was not reproducible. Also, all rescued viruses produced infectious viruses with similar kinetics after infection of the MRC5 cells at an MOI of 0.01 (Fig. 3.4D). These results suggested that both the NSm and the 78kDa proteins are not necessary for viral replication in mosquito cells as well as interferon-competent mammalian cells.

**Comparison of viral fitness of arMP-12 and arMP-12-delNSm/78**

A competition-propagation assay was performed to compare the relative fitness of arMP-12 and arMP-12-delNSm/78. Five different mixtures of arMP-12 and arMP-12-delNSm/78 were prepared at ratios of 1 to 100, 1 to 50, 1 to 20, 1 to 1, or 100 to 1 and independently inoculated into Vero E6 cells at an MOI of 0.1. At 48 h p.i., released-virus samples were collected and inoculated into Vero E6 cells at an MOI of 0.1. This method of virus passage was repeated five times. As controls, arMP-12 and arMP-12-delNSm/78 were independently passed using the same method. If arMP-12 expressing NSm and 78-kDa protein is more fit than arMP-12-delNSm/78 lacking both proteins, then it should become the major virus population during serial passage.

**A.** Vero Cells (MOI: 1.0)
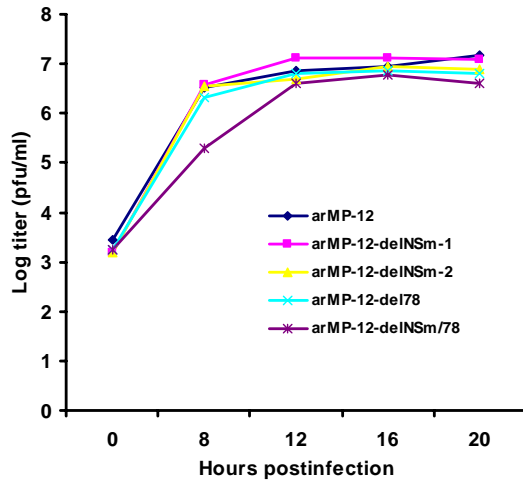


**B.** C6/36 Cells (MOI: 1.0)
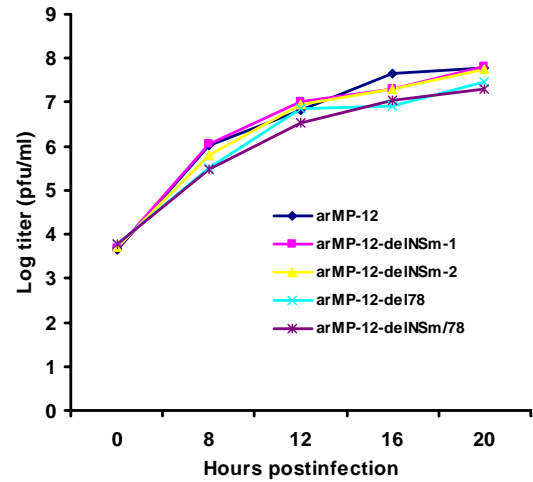


**C.** MRC5 cells (MOI: 1.0)
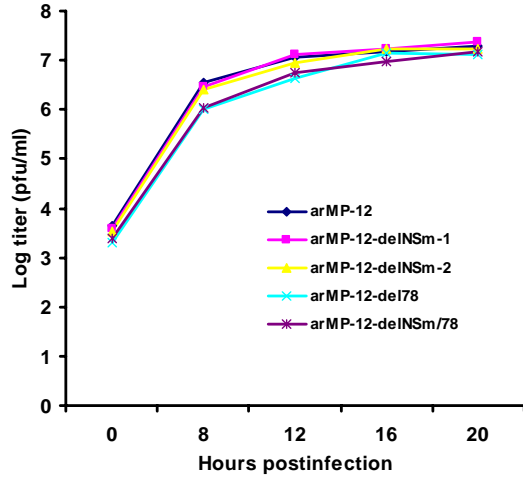


**D.** MRC5 cells (MOI: 0.01)
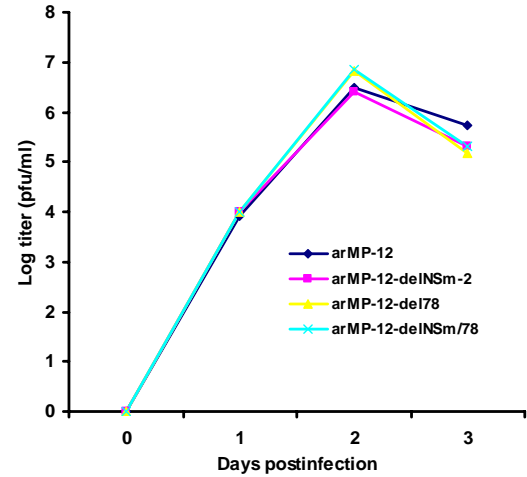


Figure 3.4: Growth curves of arMP-12 and its mutant viruses in Vero cells, C6/36 cells, and MRC5 cells

46

To estimate the abundance of arMP-12 and arMP-12-delNSm/78 in the passaged samples, intracellular RNAs were extracted from coinfected Vero E6 cells, cells infected with passage-level-three samples, and cells infected with passage-level-five samples. Then, the 159-bp-long reverse transcription-PCR product corresponding to the 5' end of antiviral-sense M segment RNA was obtained using primers M18F and M159R (Illustration 3.2). The PCR products were digested with EcoR I and then analyzed using 2% agarose gel electrophoresis (Fig. 3.5). I expected that the PCR product from arMP-12-delNSm/78, but not from arMP-12, would be sensitive to EcoR I, resulting in the generation of 140-bp and 19-bp fragments, because the 5'-end of antiviral-sense M segment RNA of arMP-12-delNSm/78 had an *EcoR*I site (Illustration 3.2). Consistent with this expectation, *EcoR*I digestion of the PCR product from the pPro-T7-avM(+)-*EcoR*I plasmid encoding the arMP-12-delNSm/78 M segment RNA and that from arMP-12-delNSm/78-infected cells both yielded the 140-bp fragment, while the 159 bp-long PCR product from plasmid pPro-T7-avM(+) and that from the arMP-12-infected cells were resistant to the *EcoR*I digestion (Fig. 3.5). Analysis of the coinfected samples showed that the ratio of the 159-bp PCR product amount to the 140-bp PCR fragment amount roughly correlated to that of input arMP-12 to input arMP-12-delNSm/78 (Fig. 3.5, P0) and there was a trend for this ratio to increase after passage. This trend was most obvious in the sample that used the initial two-virus mixture at a ratio of 1:1; the abundance of the arMP-12-delNSm/78-derived PCR fragment quickly decreased after passage (Fig. 3.5, 1:1). These data suggested that there was a slight loss of fitness for growth in cell culture for arMP-12-delNSm/78 compared to that for intact arMP-12.
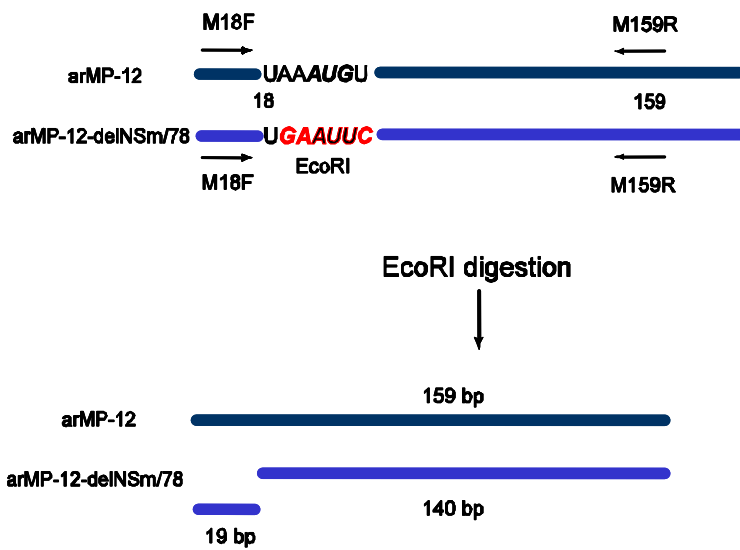
Illustration 3.2: Strategy for discrimination of arMP-12 from arMP-12-delNSm/78

Shown at the top are the structures of the 5' end of the antigenomic-sense M segment of arMP-12 and that of the arMP-12-delNSm/78 and binding sites of two PCR primers, M18F and M159R. EcoRI digestion of the arMP-12-delNSm/78-derived PCR product, but not of the arMP-12-dereived PCR product, generated 140- and 19-bp-long PCR fragments shown at the bottom.
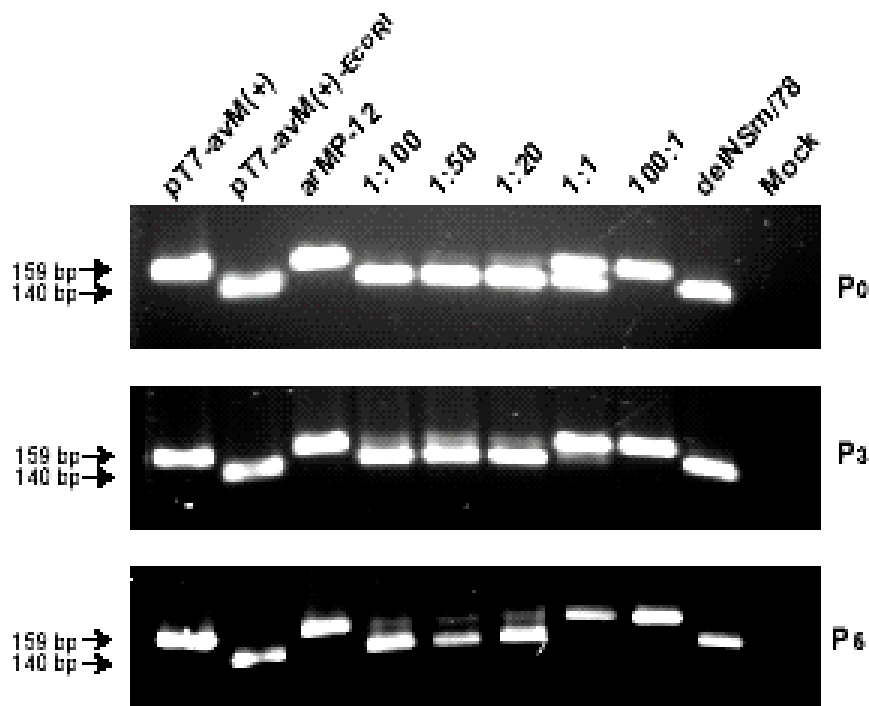
Figure 3.5: Competition-propagation assay

A competition-propagation assay was performed as described in the text. Vero E6 cells were mock-infected (Mock), independently infected with arMP-12 (arMP-12) or arMP-12-delNSm/78 (delNSm/78), or coinfected with arMP-12 and arMP-12-delNSm/78 at the indicated ratio (P0), with virus samples passaged three times (P3) or five times (P5). For extraction of intracellular RNAs, viruses were infected at an MOI of 1, while virus passage was performed at an MOI of 0.1. After synthesis of cDNA from intracellular RNAs with random hexamers, the 5' end of the antigenomic-sense M segment was amplified from these cDNAs and plasmids pPro-T7-avM(+) [pT7-avM(+)] and pPro-T7-avM(+)-EcoRI [pT7-avM(+)-EcoRI] with primer set M18F/M159R as described in Illustration 3.2. The PCR products were digested with EcoRI, and the samples were analyzed by 2 % agarose gel electrophoresis.

49

# Chapter 4: NSm Protein of Rift Valley Fever Virus Suppresses Virus-induced Apoptosis

## I. INTRODUCTION

Rift Valley fever virus (RVFV), a member of the genus *Phlebovirus* within the family *Bunyaviridae*, causes periodic outbreaks among livestock and humans in sub-Saharan African countries (109). RVFV infection results in high mortality and abortion rates in domestic ruminants with severe hepatic disease, and also causes an acute febrile myalgic syndrome, a hemorrhagic syndrome, ocular disease, and encephalitis in humans (7, 97). The most recent outbreak was reported in Kenya and resulted in a high reported case-fatality ratio in infected humans (25). Its transmission is primarily mosquito-borne or occurs due to direct contact with infected animal blood. Even though the RVFV natural infectious cycle has been linked to the *Aedes* species mosquito, many other mosquito species can be infected and subsequently transmit the virus (43), implying that multiple mosquito species can transmit the virus and increase the possibility of RVFV becoming epidemic and perhaps endemic outside its traditional area.

RVFV has a single-stranded, tripartite RNA genome composed of the L, M, and S segments. The L segment is of negative polarity encoding the RNA-dependent RNA polymerase (L). The S segment uses an ambisense strategy for gene expression; a nonstructural protein, NSs, is translated from viral-sense mRNA, while the nucleocapsid (N) protein is expressed from antiviral-sense mRNA (109). The NSs protein has been known as an interferon antagonist due to its shutting off of host transcription (12, 78). The anti-viral-sense M segment encodes two envelope glycoproteins, Gn and Gc, and two accessory proteins, 14-kDa NSm and 78-kDa. The M gene open reading frame (ORF) in

M mRNA contains five in-frame translation initiation codons within the preglycoprotein (pre-Gn) region, which exists upstream of the Gn and Gc genes (47, 61, 124). The 78-kDa protein is translated from the first AUG of the ORF, and its coding sequence includes the entire NSm and Gn coding sequences. NSm gene comprises the region that starts from the second AUG to the end of the pre-Gn region (Fig. 4.1A). The NSm and 78-kDa proteins are not essential for RVFV replication in cell culture as described in Chapter 3, whereas all RVFVs thus far sequenced carry the Pre-Gn region (14), strongly suggesting that there is selection pressure(s) to retain RNA element(s) in the pre-Gn region and/or proteins encoded in the pre-Gn region, i.e., NSm and 78-kDa protein. Currently, the biological functions of the NSm and 78-KDa proteins of RVFV and proteins encoded in the pre-Gn region of other phleboviruses are totally unclear, while a mutant RVFV lacking both NSm and 78-kDa protein expression showed an attenuated virulence in rats (13), implying a possible role of the RVFV NSm and/or 78-kDa proteins in viral pathogenesis.

In the study described in this chapter, I have generated a deletion mutant of the attenuated MP-12 strain of RVFV, which expressed neither the NSm protein nor the 78-kDa protein, due to a large deletion in the pre-Gn region of the M segment. It was found that cells infected with the deletion mutant underwent apoptotic cell death earlier than did the parental virus-infected cells, and NSm expression inhibited the rapid apoptotic cell death in the mutant virus-infected cells. NSm expression also suppressed staurosporine (STP)-induced apoptosis, demonstrating that NSm exerted its antiapoptotic function in the absence of other viral proteins. This is the first demonstration of the biological function of the NSm protein of any Phlebovirus.

51

## II. MATERIALS AND METHODS

### Cells and viruses

Vero E6 cells, human embryonic kidney 293 cells and murine macrophage-like cell line J774.1 cells were maintained in Dulbecco's modified minimum essential medium (DMEM) supplemented with 10% fetal bovine serum (FBS), penicillin (100 U/ml) and streptomycin (100 μg/ml). BHK/T7-9 cells which express T7 RNA polymerase (58) were grown in MEM-alpha containing 10% FBS. arMP-12, a recombinant vaccine candidate strain MP-12 of RVFV and arMP-12-del21/384, carrying a deletion in the pre-Gn region of arMP-12, were generated using a RVFV reverse genetics system as described in Chapter 2 and 3. Both viruses were grown, and their titers were determined by a plaque assay in Vero E6 cells.

### Plasmids and rescue of mutant virus

The entire NSm ORF (nucleotide [nt] 135 to 479 of the antiviral-sense M segment), 78-kDa ORF (nt 21 to 2090 of the antiviral-sense M segment) and 73-kDa (nt 174 to 2090 of the antiviral-sense M segment) ORF were independently cloned into a pCAGGS plasmid (63), resulting in pCAGGS-NSm, pCAGGS-78 and pCAGGS-73, respectively. For generation of pCAGGS-78, the second and third AUGs of 78-kDa ORF were substituted with GCC to eliminate expression of the NSm and 73-kDa proteins. For generation of arMP-12-del21/384, two *EcoR*I sites were created at nt numbers 21 and 384 of the M gene ORF of a plasmid expressing an anti-viral sense M segment. *EcoR*I digestion of this plasmid and subsequent self-ligation resulted in pPro-T7-avM(+)-del21/384. arMP-12-del21/384 was recovered from BHK/T7-9 cells that were

cotransfected with pPro-T7-avM(+)-del21/384, pPro-T7-avS(+), pPro-T7-avL(+), all of which express full-length antiviral-sense RNA segments, pT7-IRES-vN expressing N protein, pT7-IRES-vL expressing L protein, and pCAGGS-vG expressing proteins encoded in the M gene ORF as described in previous chapters. Rescued virus was amplified once in Vero E6 cells and used in the experiments.

**Plaque assay**

After virus adsorption to VeroE6 cells at 37˚C for 1 hr, the inoculum was removed, and the cells were washed three times with PBS and overlaid with modified Eagle's medium containing 0.6% tragacanth gum (MP Biomedicals, inc.), 2.5% FBS, and 5% tryptose phosphate broth (TPB). At 4 days postinfection (p.i.), the overlay was removed, and cells were fixed and stained with 0.75% crystal violet, 10% formaldehyde, and 5% ethanol.

**Northern blot analysis**

Intracellular RNAs were extracted from virus-infected cells using TRIzol Reagent (Invitrogen). Approximately 100 ng of RNA was denatured and separated on 1% denaturing agarose-formaldehyde gels and transferred onto a nylon membrane (Roche Applied Science). Northern blot analysis was performed with strand-specific RNA probes as described previously in Chapter 2.

**Antibodies**

Anti-NSm rabbit polyclonal antibody and polyclonal mouse anti-RVFV antibody were used to detect viral proteins as shown in Chapter 3. Anti-L protein peptide rabbit polyclonal antibody was prepared by immunizing rabbits with the synthetic peptide N-RDRSKQPFSPDHD, corresponding to amino acids 434 to 446 of the L protein.

**Western blot analysis**

Virus-infected and mock-infected cells were lysed with a sample buffer and subjected to sodium dodecyl sulfate-polyacrylamide gel electrophoresis (SDS-PAGE). The separated proteins were transferred to a polyvinylidene difluoride (PVDF; BioRad) membrane. After blocking for 1 h, the membranes were incubated with primary antibody overnight at 4˚C and with secondary antibody for 1 h at room temperature. The membrane was developed with an enhanced chemiluminescence (ECL) kit (Amersham Biosciences).

**Radioimmunoprecipitation (RIP)**

Virus-infected cells and mock-infected cells were radiolabeled with 100 μCi/ml of Trans $^{35}$S-label (MP Biomedicals) at 8 h p.i., for 30 min. Cytoplasmic extracts were prepared and incubated with anti-NSm antibody or preimmune serum. RIP was performed as described in Chapter 3.

## Cell viability assay

Confluent Vero E6 cells grown in 24-well plates were mock infected or independently infected with arMP-12 and arMP-12-del21/384 at a multiplicity of infection (MOI) of 10. Cell viability was determined by using an MTT (3-[4,5-dimethylthiazol-2-yl]-2,5-diphenyl tetrazolium bromide)-based in vitro toxicology assay kit (Sigma), which measures the activity of mitochondrial dehydrogenases in living cells. At various times p.i., MTT (0.5 mg/ml) was added to each well for 4 h, and the reaction was terminated by adding an MTT solubilization solution. After dissolving MTT formazan crystals completely, the absorbance of samples was measured at a wavelength of 570 nm, and the background absorbance at 690 nm was subtracted. Cell viability in infected cells was determined as the percentage of cell viability of mock-infected cells at the corresponding times p.i.

## Annexin-V/propidum iodide (PI) staining and flow cytometry

Vero E6 Cells were mock-infected or independently infected with arMP-12 and arMP-12-del21/384 at an MOI of 3. All cells, including floating cells, in the cultures were collected at 20 h p.i. and 40 h p.i. The harvested cells were washed three times and then stained with Annexin-V-FITC and PI for 15 min at room temperature using Annexin-V-FITC apoptosis detection kit I (BD Pharmingen). Then, $1\times10^4$ stained cells were analyzed by flow cytometry (BD FACSCanto flow cytometer, Becton Dickinson).

## Caspase enzymatic activity assays

The caspase enzymatic activities of virus-infected cells were evaluated via caspase colorimetric assay kits (BioVision, Mountain View, CA). In this assay,

approximately $1\times10^6$ cells were washed with PBS and lysed with 50 μl of chilled cell lysis buffer for 10 min on ice. After centrifugation for 1 min at 10,000 × g, supernatants (cytosolic extracts) were collected and protein concentration measured by the Bradford assay.  Fifty or one hundred micrograms of proteins were diluted in 50 μl of cell lysis buffer and 50 μl of 2×Reaction buffer for each assay. Each caspase activity was determined with colorimetric peptide substrates for caspase-3/7 (DEVD-$p$NA; chromophore $p$-nitroanilide), caspase-8 (IETD-$p$NA) and caspase-9 (LEHD-$p$NA). Each sample was incubated with the peptide substrate for 2 h, and color changes were measured at 405 nm in a spectrophotometer using a quartz microcuvette. Background reading from cell lysates and buffers was subtracted from the sample reading.

**Reagents**

Anti-cleaved caspase-3 (Asp175) antibody and anti-poly ADP-ribose polymerase (PARP) antibody were purchased from Cell Signaling Technology (Danvers, MA). Staurosporine and DMSO were obtained from Sigma Aldrich (St. Louis, MO) and Z-IETD-FMK (caspase-8 inhibitor) and Z-LEHD-FMK (caspase-9 inhibitor) were purchased from BD Biosciences (San Jose, CA).

**Statistical analysis**

A paired Student's $t$ test was used to compare significance. A $p$ value of less than 0.05 was considered statistically significant.

## III. RESULTS

**Generation of arMP-12-del21/384 carrying a large deletion in the pre-Gn region of the M segment**

The pre-Gn region of RVFV M gene ORF contains five in-frame start codons, and the 78-kDa and NSm proteins are translated from the first and second AUG, respectively (Fig. 4.1A) (61, 124, 133). In Chapter 3, it is described that neither the 78-kDa protein nor the NSm protein is detected in cells infected with arMP-12-delNSm/78 that carries substitution mutations in the first and second AUGs. This mutant virus and the parental virus arMP-12 form plaques similar in size and morphology, and both have comparable growth kinetics in several cell lines. I, however, unexpectedly detected an additional protein(s) having a 73- to-75-kDa molecular mass, which is recognized by the anti-NSm antibody, in arMP-12-delNSm/78-infected cells and in arMP-12-infected cells. To completely eliminate accumulation of detectable viral proteins whose coding sequences contain the pre-Gn region in virus-infected cells, I generated another mutant virus, arMP-12-del21/384, with a deletion from nucleotides 21 to 384 in the pre-Gn region by using a reverse genetics system (Fig. 4.1A). Sequence analysis showed that the rescued arMP-12-del21/384 retained the introduced deletion in the pre-Gn region and had no other mutations in the M segment. In contrast to arMP-12-delNSm/78 that produces indistinguishable plaques from those made by arMP-12, arMP-12-del21/384 produced plaques that were larger than those produced by arMP-12 in Vero E6 cells (Fig. 4.1B). I have successfully recovered arMP-12-del21/384 in three independent rescue experiments and all rescued viruses produced plaques that were similar in size and morphology;

however, they were larger than arMP-12's plaques, suggesting that the larger plaque
phenotype was caused by the introduced deletion within the pre-Gn region.
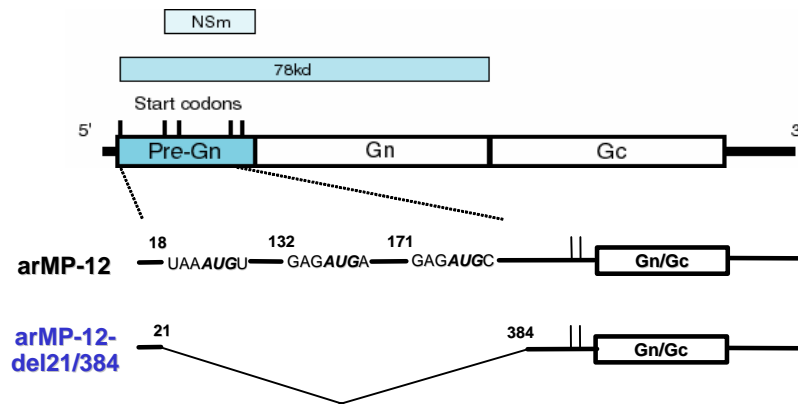


Illustration 4.1: Schematic diagram of antigenomic-sense M segment of arMP-12 and
arMP-12-del21/384

The vertical lines in the pre-Gn region represent five in-frame translation initiation
condons. Coding regions of the NSm and 78-kDa proteins are illustrated as two boxes at
the top of the diagram. The sequences around the first, second, and third AUGs and the
deleted region of pre-Gn in arMP-12-del21/384 are shown at the bottom of the diagram.

arMP-12                    arMP-12-del21/384
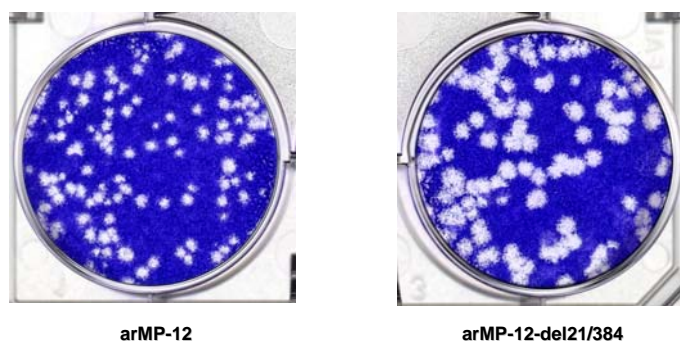
Figure 4.1: Plaque morphology of arMP-12 and arMP-12-del21/384

Vero E6 cells were infected with arMP-12 and arMP-12-del21/384, and plaques were fixed and stained with 0.75 % crystal violet, 10 % formaldehyde, and 5 % ethanol at 4 days p.i.

**Analysis of accumulation of viral RNAs and proteins and growth kinetics of arMP-12-del21/384**

Northern blot analysis revealed the accumulation of similar levels of viral-sense RNAs in arMP-12-infected and in arMP-12-del21/384-infected Vero E6 cells (Fig. 4.2A). Both viruses also accumulated similar amounts of anti-viral sense RNAs (data not shown). Western blot analyses showed that there were no substantial differences in the amounts of L, Gn/Gc, NSs and N proteins between arMP-12-infected and arMP-12-del21/384-infected Vero E6 cells (Fig. 4.2B); a modest increase in the accumulation of Gn/Gc, N and NSs proteins in arMP-12-del21/384-infected cells relative to arMP-12-infected cells shown in Fig. 4.2B was not reproducible. Radioimmunoprecipitation (RIP) analysis of infected cell lysates by anti-NSm antibody showed accumulations of 78-kDa

59

protein, NSm protein and a viral protein with a molecular mass of 75-kDa (75-kDa protein) in arMP-12-infected cells, whereas accumulations of these proteins did not occur in arMP-12-del21/384-infected cells (Fig. 4.2B and 4.2C). A similar RIP analysis of the arMP-12-delNSm/78-infected cells demonstrated selective immunoprecipitation of a viral protein with a molecular mass of 73k-Da (73-kDa protein, Fig 4.2C). arMP-12 and arMP-12-del21/384 showed similar growth kinetics in Vero E6 cells after infection at an MOI of 1 (Fig. 4.3A). They also replicated with similar kinetics in 293 cells, MRC-5 cells and murine macrophage-like cell line J774.1 cells (8) after infection at an MOI of 1 as well as 0.01 (Fig. 4.3B – 4.3D, and data not shown). These data were consistent with previous findings that the lack of NSm and 78-kDa protein accumulation as well as the presence of a large deletion at the pre-Gn region do not affect virus replication efficiency in cell cultures, as described in Chapter 3 (45).

**arMP-12-del21/384 replication induces extensive apoptotic cell death compared to arMP-12 replication**

arMP-12-del21/384 and arMP-12 replicated with similar kinetics in cell cultures; yet the former produced larger plaques than did the latter (Fig. 4.1 and 4.3). These data led me to hypothesize that arMP-12-del21/384 replication induces more extensive cell death than does arMP-12 replication. To test this hypothesis, Vero E6 cells were independently infected with arMP-12, arMP-12-delNSm/78, and arMP-12-del21/384 at an MOI of 10, and cell viabilities were determined by an MTT-based cytotoxicity assay that measures the mitochondrial dehydrogenase activities of live cells. Cell viabilities of infected cell cultures were expressed as percentages of the absorbance of a mock-infected
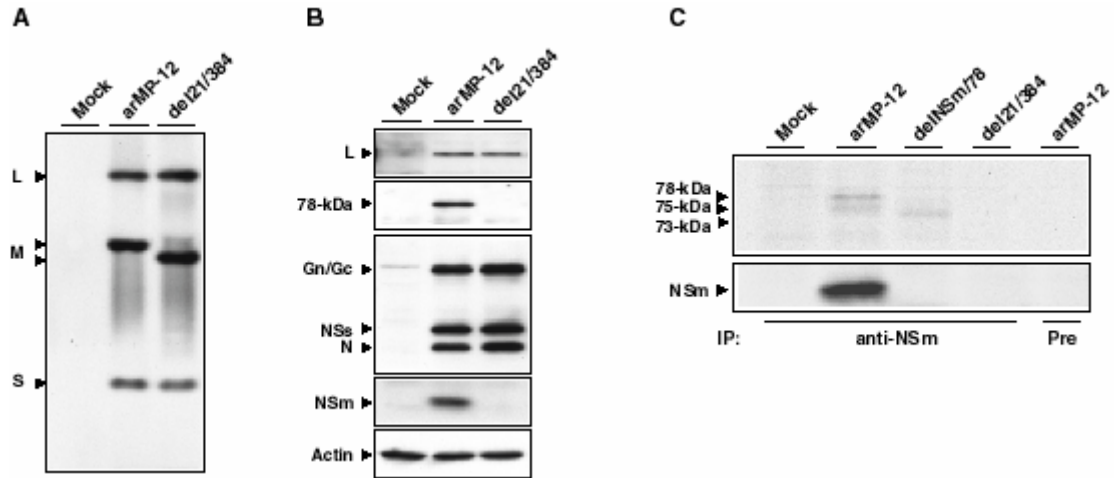
Figure 4.2: Analysis of viral RNAs and proteins of arMP-12 and arMP-12-del21/384

(A) Vero E6 cells were mock-infected (Mock) or independently infected with arMP-12 and arMP-12-del21/384 at an MOI of 1. Intracellular RNAs were extracted at 8 h p.i., and the accumulation of viral RNA was examined by Northern blot analysis with viral-sense-specific RNA probe as described in Chapter 2. L, M, and S segments are indicated with arrowheads. The M segment of arMP-12-del21/384 migrated faster than that of arMP-12 due to a large deletion in the pre-Gn region. (B) Vero E6 cells were mock-infected (Mock) or independently infected with indicated viruses at an MOI of 3, and total proteins were collected at 8 h p.i. Western analysis using anti-RVFV antibody was performed to demonstrate the accumulation of the Gn/Gc, NSs, and N proteins. Anti-L antibody and anti-actin antibody were used to detect the L protein, and actin protein, respectively, while anti-NSm antibody was used to detect both the NSm and 78-kDa proteins. (C) Vero E6 cells were mock infected (Mock) or independently infected with the indicated viruses at an MOI of 3. Cells were radiolabeled with 100 µCi/ml at 8 h p.i. for 30 min. Cytoplasmic extracts were incubated with anti-NSm antibody (anti-NSm) or preimmune serum (Pre), and radioimmunoprecipitation was performed as described previously.

61

**A.** Vero E6 cells (MOI: 1.0)

**B.** 293 cells (MOI: 1.0)

**C.** J774.1 cells (MOI: 1.0)

**D.** J774.1 cells (MOI: 0.01)
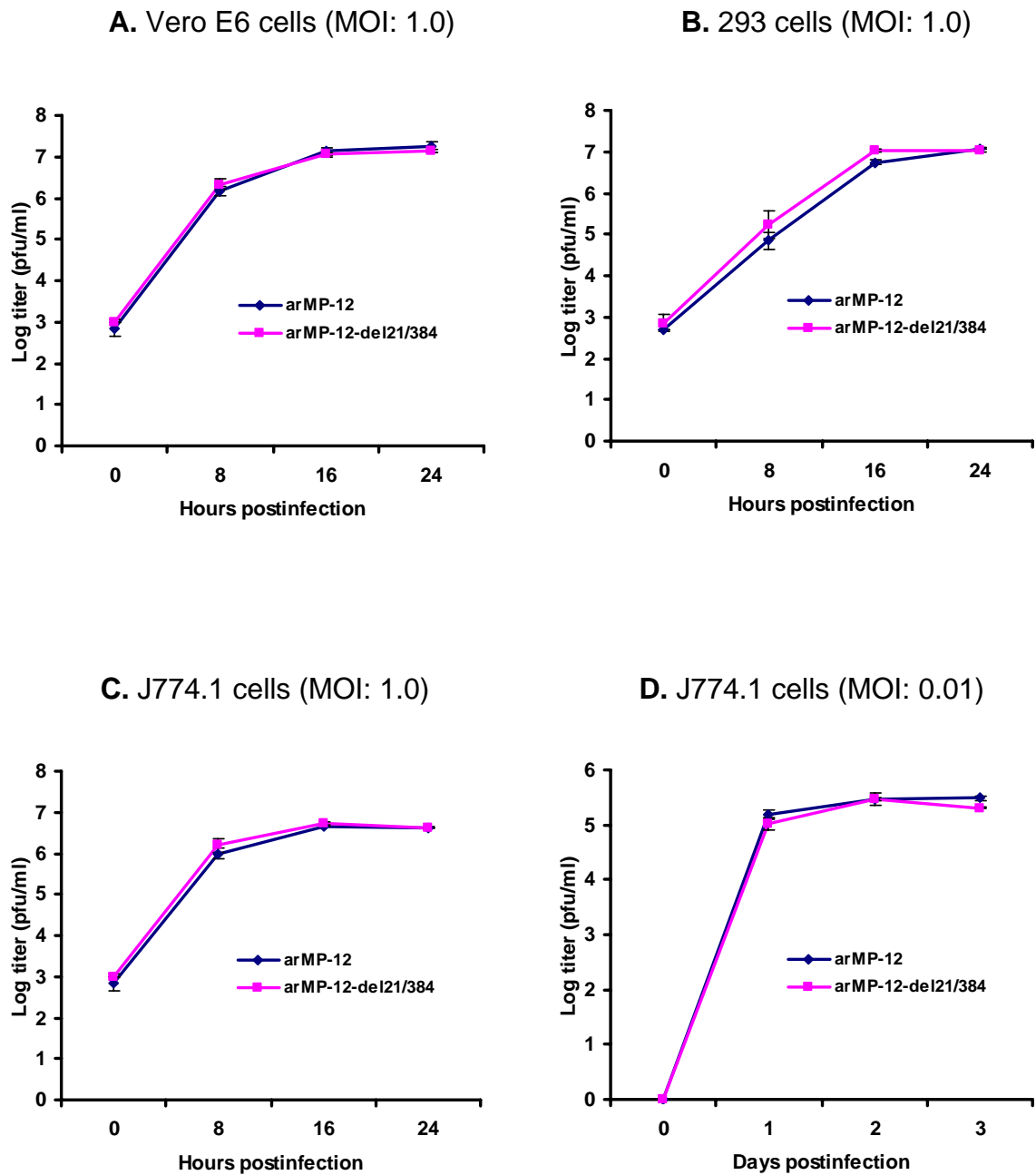
Figure 4.3: Growth kinetics of arMP-12 and arMP-12-del21/384 in Vero E6 cells, 293 cells, and J774.1 cells

cell culture at the corresponding times p.i. (Fig. 4.4). All infected cell cultures showed similar levels of cell viabilities during the first 24 h p.i., whereas cell viabilities in arMP-12-del21/384-infected cells were significantly lower than those in arMP-12-infected cells from 48 h p.i. to 72 h p.i.; at 60 h p.i., the cell viability of arMP-12-del21/384-infected cultures was about 40 % less than those of arMP-12-infected cell cultures. Kinetics of cell viability between arMP-12-delNSm/78-infected cells and arMP-12-infected cells was similar throughout infection, except at 24 h p.i., where marginally less cell viability was observed in the former.

To determine whether arMP-12-del21/384 replication induced a more extensive apoptotic cell death than did arMP-12 replication, Annexin-V/propidium iodide (PI) staining and subsequent flow cytometry analysis were performed. Annexin-V is a $Ca^{2+}$-dependent phospholipid-binding protein with a high affinity for the phosphatidylserine, which is translocated from the inner to the outer leaflet of the plasma membrane in the early stages of apoptosis (86). PI, which intercalates into double-stranded DNAs, is excluded by viable cells but can penetrate cell membranes of dying or dead cells (130). Accordingly, Annexin-V-positive and PI-negative cells are those undergoing early apoptosis. Vero E6 cells were mock infected or independently infected with arMP-12 and arMP-12-del21/384 at an MOI of 3. An immunofluorescence assay that detected viral proteins showed that nearly 100% of Vero E6 cells and 293 cells were infected with viruses at an MOI of 3 (data not shown). At 20 h and 40 h p.i., all cells, including floating cells, were collected from the cultures and stained with Annexin-V/PI, and then analyzed by flow cytometry (Fig. 4.5); the lower right quadrant (Q4) represents early apoptotic cells, i.e., Annexin-V-positive and PI-negative cells.
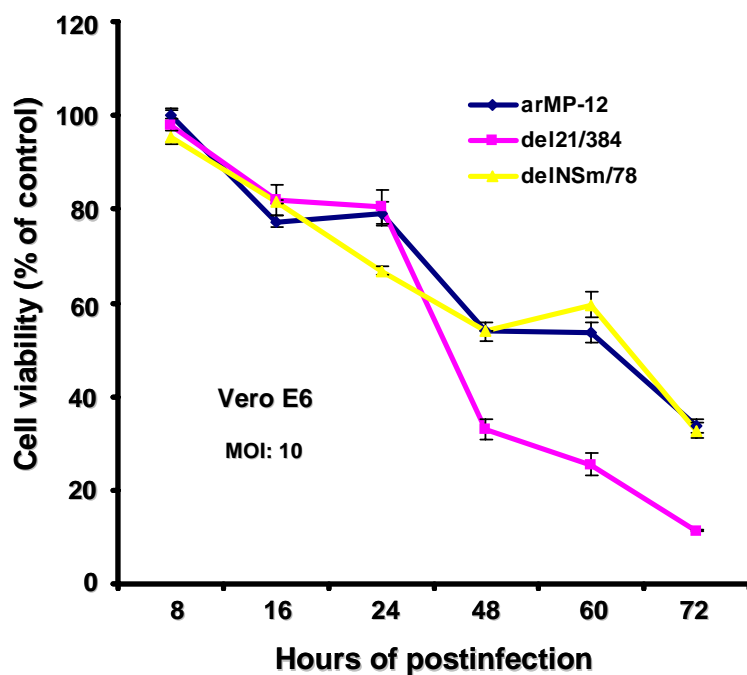
Figure 4.4: Cell viability assay

Vero E6 cells were independently infected with arMP-12, arMP-12-delNSm/78 and arMP-12-del21/384 at an MOI of 10. At the indicated h p.i., infected cells were treated with 0.5 mg/ml of MTT and incubated for 4 h. The metabolic reaction was terminated, and MTT formazan crystals in living cells were dissolved by adding an MTT solubilization solution. The absorbance was measured at a wavelength of 570 nm and subtracted by the background absorbance at 690 nm. Cell viability was calculated by the percentage of mock-infected control of the corresponding times p.i. The data are the result of triplicate experiments.

At 20 h p.i., mock-infected cells and arMP-12-infected cells had 5.9% and 8.4% apoptotic cells, respectively, whereas 20.7% of the cells underwent apoptosis in arMP-12-del21/384-infected cells, demonstrating that the number of cells at the early state of apoptosis was substantially higher in arMP-12-del21/384-infected cells than in arMP-12-infected cells. At 40 h p.i., the apoptotic cell populations increased substantially in infected cells, while the apoptotic cell population in arMP-12-del21/384-infected cells (35.6%) was higher than that in arMP-12-infected cells (22.3%). Furthermore, the population of cells at the late stages of apoptosis and/or necrosis, which are shown in the upper right quadrant (Q2), increased in infected cells by 40 h p.i., and the population of these cells in arMP-12-del21/384-infected cells (24.2%) was higher than the corresponding cell population of arMP-12-infected cells (14.8%). These data suggested that the NSm and/or 78-kDa proteins suppressed virus-induced apoptotic cell death.

**Status of caspase activation in arMP-12-infected cells and in arMP-12-del21/384-infected cells**

It is well established that once apoptosis is triggered, upstream caspases, e.g., caspase-8 or -9, induce the cleavage of caspase-3, yielding active cleaved forms of caspase-3 (p17/p19), which in turn cleaves the downstream cellular substrates, e.g., poly(ADP-ribose) polymerase (PARP) to execute apoptosis (75). To further establish that arMP-12-del21/384 replication induced apoptotic cell death more readily, and which was more extensive than that induced during arMP-12 replication, I examined the activation status of caspase 3 in arMP-12-infected cells and in arMP-12-del21/384-infected cells.
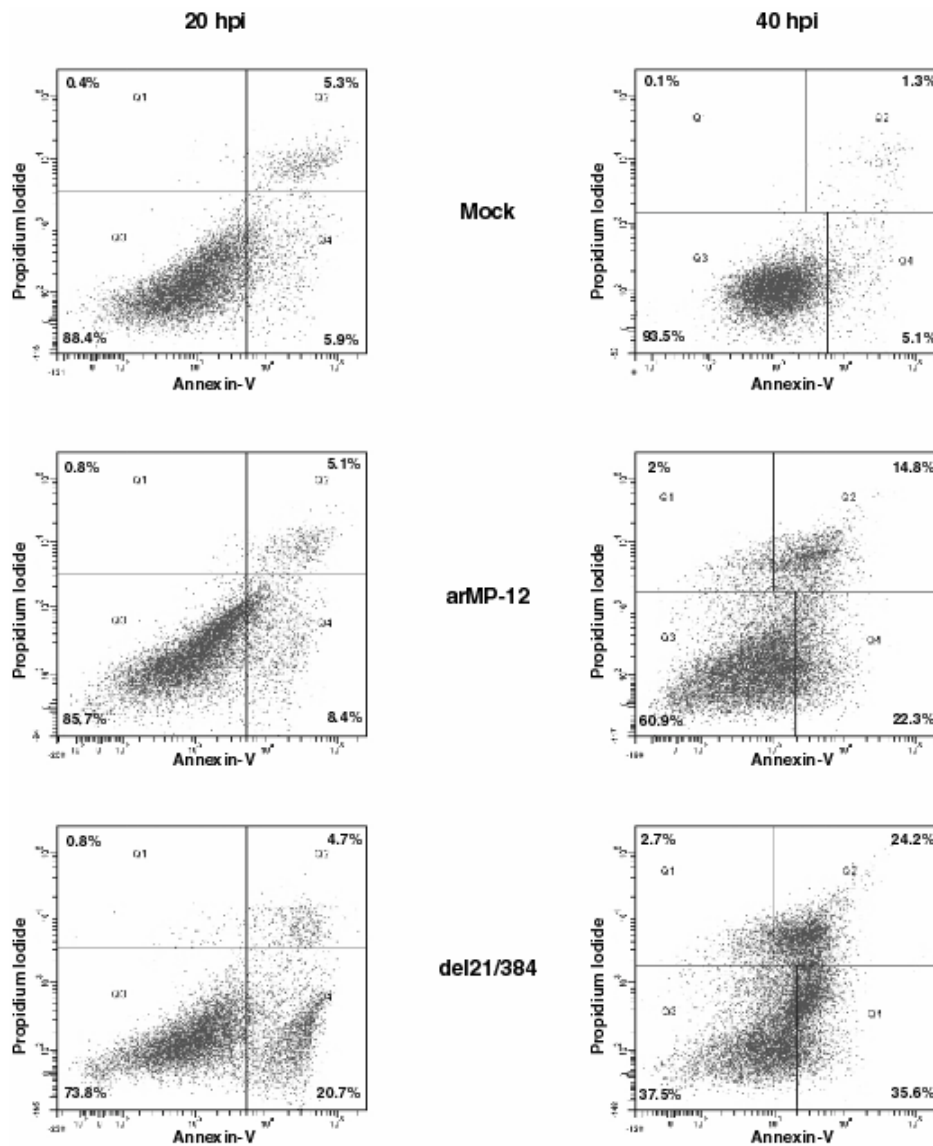
Figure 4.5: Annexin-V/PI staining and flow cytometric analysis

Vero E6 cells were mock-infected (Mock) or independently infected with arMP-12, and arMP-12-del21/384 at an MOI of 3. Cells, including floating cells, were collected at 20 h p.i. and 40 h p.i., and stained with Annexin-V and PI for 15 min. $1\times10^4$ stained cells were analyzed by flow cytometry. Dot plots are divided into quadrants of cell populations: Q1 (staining PI positive, Annexin-V negative), Q2 (staining both positive), Q3 (staining both negative), and Q4 (staining Annexin-V positive, PI negative). The percentages of the cells in each quadrant are also presented.

66

Vero E6 cells, 293 cells and J774.1 cells were mock infected or independently infected with arMP-12 and arMP-12-del21/384 at an MOI of 3, and cell lysates were collected at 8, 16 and 24 h p.i. for Vero E6 and 293 cells; the majority of cells were attached in flasks at 24 h p.i. in infected Vero E6 and 293 cell cultures. In contrast, a majority of cells at 24 h p.i. in the infected J774.1 cell cultures were detached from the flasks, suggesting that most of the infected cells were dead by 24 h p.i. Hence, cell extracts were prepared at 2, 4, 6 and 8 h p.i. from infected J774.1 cells. Cell lysates were subjected to Western blot analysis to assess levels of caspase-3 cleavage and cleavage of its downstream substrate, PARP (Fig. 4.6). Staurosporine (STP), which is a broad-spectrum protein kinase inhibitor that has been used to induce apoptosis in various cell lines (50, 74, 119), served as a positive control for the apoptosis inducer. As shown in Fig. 4.6, STP treatment induced accumulations of cleaved caspase-3 and PARP, while neither was accumulated in DMSO-treated cells. In both 293 and Vero E6 cells, throughout infection, the amount of cleaved caspase-3 was more abundant in arMP-12-del21/384-infected cells than in arMP-12-infected cells. In 293 cells, caspase-3 cleavage was detected as early as 8 h p.i. in arMP-12-del21/384-infected cells, whereas only a low level of cleaved caspase-3 was detectable at 16 h p.i. in arMP-12-infected cells. Likewise, the levels of PARP cleavage were more extensive in the mutant virus-infected cells than in parental arMP-12-infected cells. I also noted efficient accumulations of the cleaved caspase-3 and PARP at 6 h p.i. in arMP-12-del21/384-infected J774.1 cells, but not in arMP-12-infected J774.1 cells, whereas these differences were no longer obvious at 8 h p.i. (Fig. 4.6B). Western blot using anti-RVFV antibody showed that accumulation of N and NSs proteins was similar between arMP-12-infected cells and arMP-12-del21/384-infected cells, which, with the identical growth curves (Fig. 4.3), suggested

67

**A.**

**Vero E6**

**293**

**B.**

**J774.1**

68
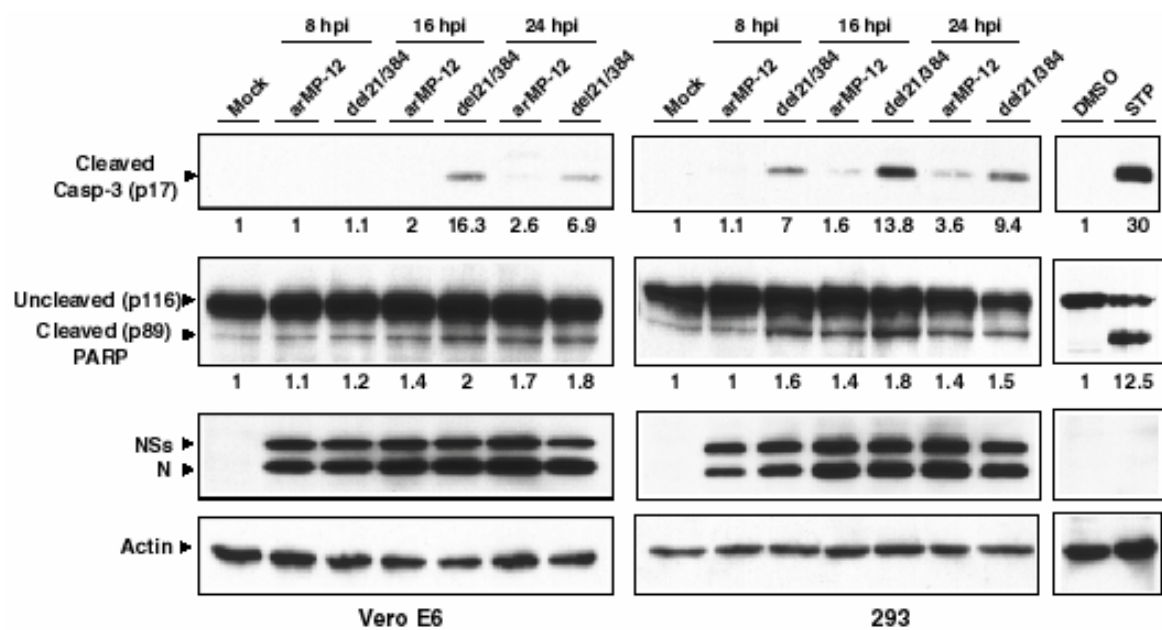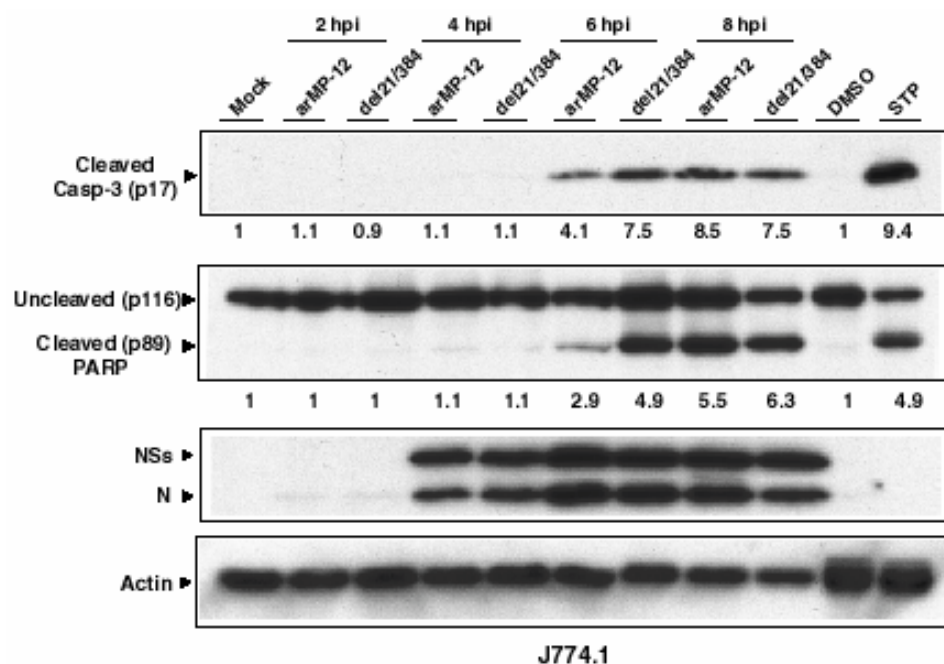
Figure 4.6: Activation of caspase-3 and cleavage of PARP in virus-infected cells

Vero E6, 293 (A) and J774.1 (B) cells were mock infected (Mock) or infected with arMP-12 and arMP-12-del21/384 at an MOI of 3. Total cell lysates were collected at the indicated h p.i. and subjected to Western blot analysis.  Anti-cleaved caspase-3 (Asp175), anti-PARP antibody and anti-actin antibody were used to demonstrate cleaved caspase-3 (p17), both uncleaved and cleaved PARP and actin, respectively. RVFV N and NSs proteins were detected by anti-RVFV antibody. STP and DMSO represent the 293 cells that were treated with 3 μM of STP in DMSO and with DMSO only, respectively.  The specific band signal in each immunoblot was quantified by densitometric scanning and normalized against actin control for the cleaved caspase-3 or against total PARP (uncleaved and cleaved PARP) for the cleaved PARP.  The fold increase over the signal from mock-infected cells is indicated below each lane.

that increased caspase-3 activation in arMP-12-del21/384-infected cells was not due to the more efficient replication of this virus.

To further confirm that the cleaved caspase-3 in arMP-12-del21/384-infected cells was biologically active, caspase-3/7 activities in arMP-12-infected cells and in arMP-12-del21/384-infected cells were measured by using their colorimetric substrate, DEVD-$p$NA. The levels of caspase-3/7 activities in the mutant virus-infected cells were substantially higher than those of the parental virus-infected cells at 16 h p.i. in both Vero E6 and 293 cells (Fig. 4.7A) ($p < 0.001$). In contrast, only an insignificant difference in the caspase-3/7 activities was detected between mock-infected cells and arMP-12-infected cells ($p > 0.05$).

Next I determined the enzymatic activities of the upstream caspases, i.e., caspase-8 (Fig. 4.7B) and caspase-9 (Fig. 4.7C), at 16 h p.i. in infected Vero E6 and 293 cells. In both cell lines, caspase-8 activities were higher in arMP-12-del21/384-infected cells than in arMP-12-infected cells; these differences were statistically significant ($p < 0.001$). Caspase-8 activities in arMP-12-infected cells were also statistically higher than those in mock-infected cells ($p < 0.001$ in Vero E6 cells and $p < 0.005$ in 293 cells). Caspase-9 activities were statistically higher in arMP-12-del21/384-infected cells than in arMP-12-infected cells ($p < 0.05$ in both cell lines), whereas those between mock-infected cells and arMP-12-infected cells, as well as those between mock-infected cells and arMP-12-del21/384-infected cells, were not statistically significant in both cell lines. These data suggested that activated caspase-8 primarily exerted caspase-3 cleavage in arMP-12-del21/384-infected cells. Overall, our data were consistent with a notion that the viral proteins encoded in the pre-Gn region, including the NSm and/or 78-kDa proteins,

suppressed caspase-8 activities and its downstream caspase-3 activities, causing a delayed apoptotic cell death in arMP-12-infected cells.
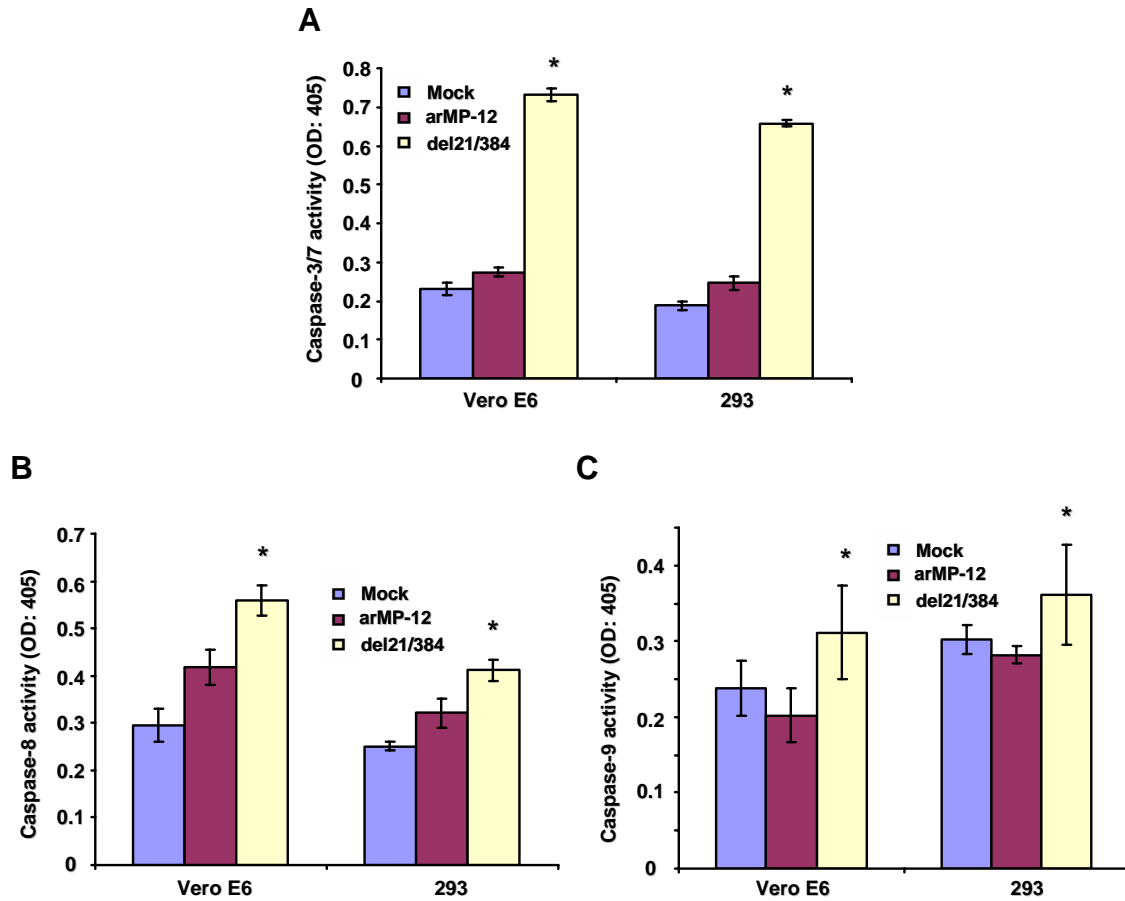


Figure 4.7: Enzymatic activities of caspases in virus-infected cells

Vero E6 and 293 cells were mock infected (Mock) or independently infected with arMP-12 and arMP-12-del21/384 at an MOI of 3. Cells were collected at 16 h p.i. and 100 µg of proteins from each sample were incubated with colorimetric peptide substrates for caspase-3/7 (A), caspase-8 (B) and caspase-9 (C) for 2 h. Color changes were measured at 405 nm and background reading from cell lysates and buffers was subtracted from the sample reading. Data are representative of at least three independent experiments and statistical significance was determined by a paired Student'$t$ test. Asterisks represent p values between arMP-12 and arMP-12-del21/384 infections ($p < 0.001$, $p < 0.001$ and $p < 0.05$ of the panel A, B and C, respectively).

**Expression of NSm and 73-kDa proteins suppresses caspase-3 cleavage and activation in arMP-12-del21/384-infected cells**

To know whether the viral proteins carrying the pre-Gn region, i.e., NSm, 73-kDa protein or 78-KDa protein, could exert apoptotic cell death inhibition in RVFV-infected cells, 293 cells were independently transfected with eukaryotic expression plasmids encoding the NSm protein ORF (pCAGGS-NSm), 78-kDa protein ORF (pCAGGS-78), 73-kDa protein ORF (pCAGGS-73) and a control plasmid, pCAGGS. In this system, transfection efficiencies achieved in 293 cells were about 70-80% (data not shown). At 48 h posttransfection, cells were mock infected or independently infected with arMP-12 and arMP-12-del21/384 at an MOI of 3. Total cell lysates were collected at 16 h p.i. and subjected to Western blot analysis to compare the level of caspase-3 cleavage (Fig. 4.8A). It was evident that transfection of pCAGGS-NSm and pCAGGS-78 resulted in efficient accumulations of NSm protein and 78-kDa protein, respectively; the abundance of NSm protein in transfected cells was higher than that in arMP-12-infected cells. Transfection of pCAGGS-73 resulted in a modest amount of 73-kDa protein accumulation. In arMP-12-infected cells (Fig. 4.8, lanes 5-8), the expression of all three proteins had little effect on the abundance of cleaved caspase-3, p17, whereas expression of the NSm and 73-kDa proteins clearly suppressed p17 accumulation in arMP-12-del21/384-infected cells (Fig. 4.8, lanes 10 and 12). In contrast, the 78-kDa protein expression had little effect on the p17 accumulation in arMP-12-del21/384-infected cells (Fig. 4.8, lane 11). Consistent with those data, casapase-3/7 activities in arMP-12-del21/384-infected cells that expressed NSm protein or the 73-KDa protein (73), but not the 78-KDa protein (78), were statistically decreased compared to those found in arMP-12-del21/384-infected cells that were transfected with pCAGGS (empty vector [EV]) ( $p < 0.001$: EV vs NSm, $p < 0.05$: EV vs 73) (Fig. 4.8B). These experiments demonstrated that independently

expressed NSm and 73-kDa proteins, but not 78-kDa protein, from the transfected plasmids worked in *trans* to suppress caspase-3 activation in arMP-12-del21/384-infected cells; NSm and 73-kDa proteins indeed exerted apoptotic cell death inhibition in RVFV-infected cells.

**A**
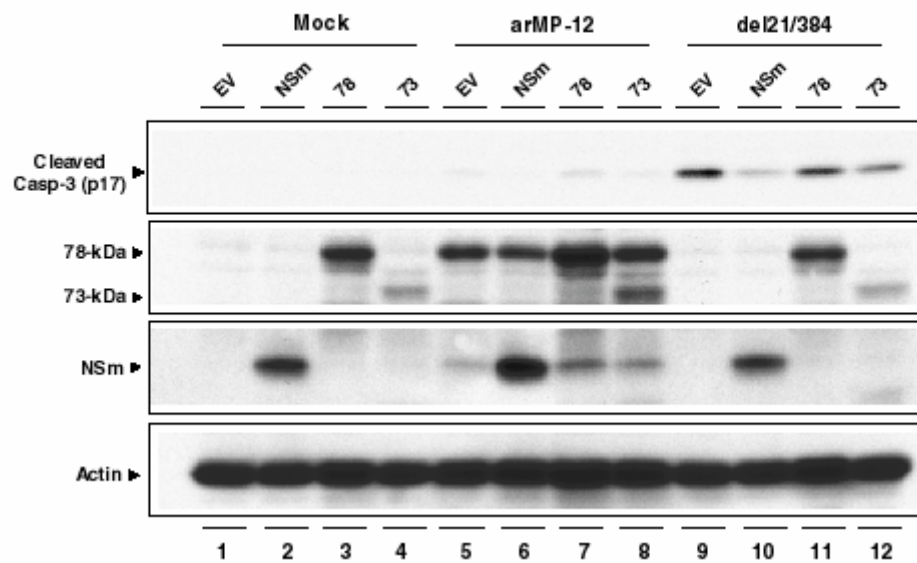


**B**
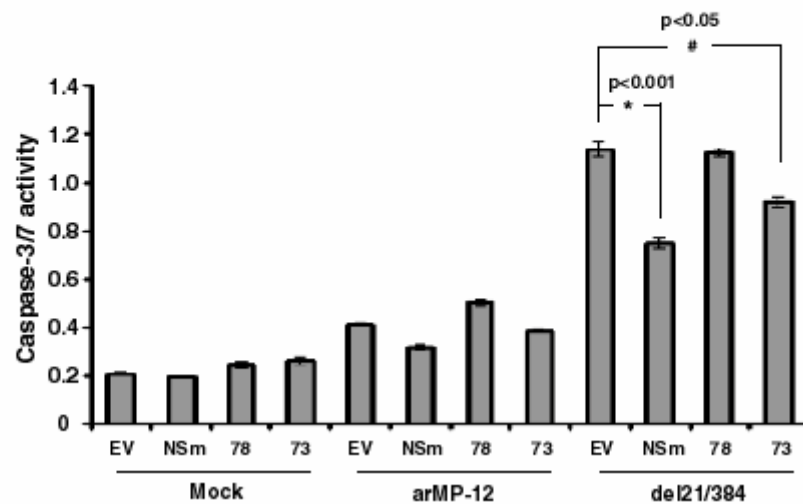
Figure 4.8: Effect of NSm expression on arMP-12-del21/384 replication-induced apoptosis

(A) 293 cells in 12-well plates were independently transfected with 1 μg of pCAGGS (EV), pCAGGS-NSm (NSm), pCAGGS-78 (78), or pCAGGS-73 (73).  At 48 h post-transfection, cells were mock-infected (Mock) or independently infected with arMP-12 and arMP-12-del21/384 (del21/384) at an MOI of 3. Total cell lysates were collected at 16 h p.i., and analyzed by Western blot analysis with anti-cleaved casapase-3 antibody detecting cleaved caspase 3, p17, anti-NSm antibody detecting NSm, 73-kDa and 78-kDa protein, and anti-actin antibody detecting actin. Experiments were performed three times and similar results were obtained.  A set of representative data is shown in A.  (B) 293 cells in 6 well-plates were transfected with 2.5 μg of plasmids as described in (A) and mock-infected (Mock) or independently infected with arMP-12 and arMP-12-del21/384 at 48 h post-transfection. At 16 h p.i., cell lysates were collected and casapase-3/7 enzymatic activity of lysates was analyzed as described in Fig 4.7. All samples were prepared in triplicate, and statistical significance was determined by a paired Student's $t$ test (*, $p < 0.001$; #, $p < 0.05$).

**NSm protein expression suppresses STP-induced apoptosis**

To further establish an anti-apoptotic function of the NSm protein, I examined whether NSm protein expression suppressed STP-induced apoptosis to further establish an anti-apoptotic function of the NSm protein; STP activates both caspase-8 and caspase-9 (119), while the exact mechanism by which STP induces apoptosis is unclear. 293 cells were independently transfected with pCAGGS and pCAGGS-NSm, followed by treatment with 3 μM of STP at 48 h posttransfection. Cell extracts were prepared at 3 h after STP treatment and the enzymatic activities of caspase-8 and caspase-9 were measured (Fig. 4.9). Consistent with my expectation, STP treatment induced activation of both caspases. It was evident that NSm protein expression efficiently suppressed STP-induced activation of both caspases-8 and 9. NSm protein was quite competent to suppress STP-induced caspases-8 and -9 activities, as its inhibitory effects were comparable to those of the synthetic caspase-8 inhibitor, Z-IETD, and caspase-9 inhibitor, Z-LEHD (Fig. 4.9A and 4.9B). These data clearly demonstrated that the NSm protein alone inhibited STP-mediated apoptosis at the levels of activation of initiator caspases, caspases-8 and -9.
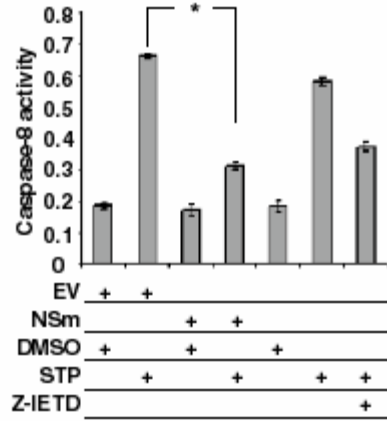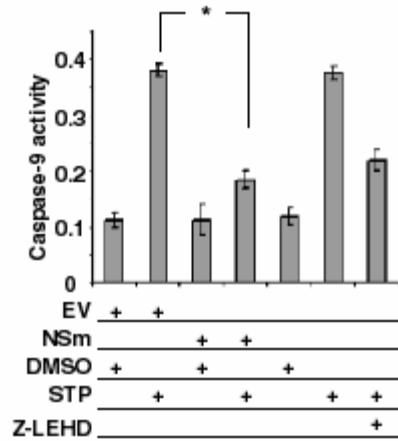
Figure 4.9: Inhibition of STP-induced apoptosis by NSm expression

293 cells were independently transfected with pCAGGS (EV) or pCAGGS-NSm (NSm), followed by the treatment of 3 μM of STP or DMSO at 48 h post-transfection. The enzymatic activities of caspase-8 (A) and caspase-9 (B) were measured with 50 μg of lysates at 3 h after treatment with STP or DMSO as described in Fig. 4.7. For controls, cells were treated with 20 μM of synthetic caspase-8 inhibitor (Z-IETD) and caspase-9 inhibitor (Z-LEHD) 1 h prior to STP treatment. Asterisks represent $p$ values in the panel A ($p < 0.001$) and panel B ($p < 0.01$). The data are the result of triplicate experiments.

# Chapter 5: Discussion and Conclusion

## I. REVERSE GENETICS SYSTEM OF RVFV

Control of RVFV after either natural introduction or bioterrorist attack would require protection of humans and livestock. Although a formalin-inactivated and lyophilized RVFV vaccine (TSI-GSD-200) has been widely used in laboratory workers (100), that immunogen is no longer available due to its requirement of several doses for boosting and high cost for production. An attenuated vaccine, MP-12 is safe and immunogenic but requires further development (24, 88). One of the critical elements of understanding the safety profile of MP-12 as a human vaccine is to understand the significance of its more than 20 point mutations for attenuation (131). This task and the additional development of an animal vaccine are critically dependent on a reverse genetics system.

Chapter 2 of this dissertation describes an RVFV reverse genetics system, the first for viruses of the *phlebovirus* genus. Infectious RVFV was consistently rescued by cotranfecting plasmids encoding anti-viral-sense RNA segments and plasmids expressing L, N, and envelope proteins into BHKT7/9 cells that stably express T7 RNA polymerase (58), while rescue of the infectious viruses did not occur after cotranfection of 293T or BHK-21 cells with pCT7pol plasmid encoding T7 RNA polymerase along with other protein-expressing and RNA-expressing plasmids (data not shown). It is unclear why virus rescue failed using transient T7 polymerase expression. When cells are cotransfected with plasmids bearing RVFV structural protein genes and a plasmid

77

expressing a viral minigenome encoding the green fluorescent protein (GFP) ORF, production of infectious virus-like particles (VLPs) carrying viral minigenome RNA was more efficient in BHK/T7-9 cells than in 293T or BHK-21 cells transiently expressing T7 polymersase, implying that virus assembly in BHK/T7-9 cells was more active than in the latter two cells. Not all BHK-derived cell lines constitutively expressing T7 polymerase were suitable for virus rescue, because no infectious viruses were obtained using BHK-21 cells expressing high levels of T7 polymerase induced by an Eastern equine encephalitis virus replicon (data not shown). Although the first reverse genetics system of BUN used vaccinia virus expressing T7 polymerase (21), all recent bunyavirus reverse genetics systems, including this study, have used BHK cells that stably express T7 polymerase without employing any virus vectors (18, 83). The mechanisms for this success are unknown, but the practical implications are obvious.

Transfection of protein expression plasmids inhibits LAC rescue (18) but has no effect on rescue of infectious BUN (83). Cotransfection of protein expression plasmids and RNA expression plasmids resulted in consistent recovery of MP-12 (Table 2.1 and 2.2). Infectious viruses were also recovered in the absence of protein expression plasmids, but virus rescue was not always successful (Table 2.1). In both BUN (21, 83) and LAC (18) reverse genetics systems, infectious viruses are produced only from cells that express anti-viral-sense RNA transcripts, whereas infectious MP-12 was recovered from cells expressing viral-sense RNA transcripts or anti-viral-sense RNA transcripts (Table 2.1). These studies indicated that requirements and optimal conditions for virus recovery vary among members of the *Bunyaviridae* family.

The establishment of a RVFV (MP-12) reverse genetics system, as described here, will facilitate molecular virology studies of RVFV, identify the role of viral cis- or

78

trans-acting elements which have not been determined, assess current vaccine candidates, produce new vaccines, and incorporate marker genes into animal vaccines. In addition, MP-12 may be developed as an expression vector that can be used for mammalian and insect cells as well as in whole animals.


## II. ACCESSORY PROTEINS, NSM AND 78-KDA PROTEINS OF RVFV


Viral proteins that are not essential for virus replication in cell culture are often called accessory proteins. The RVFV NSs protein is a such accessory protein. The mutant MP-12 lacking the NSs gene replicates as efficiently as MP-12 in Vero cells and 293 cells (55), but it does not replicate efficiently in MRC5 cells, most probably due to production of IFN β in those cells. The study in Chapter 3 of this dissertation also identified NSm and the 78-kDa protein as being RVFV accessory proteins. In contrast to an MP-12 mutant lacking the NSs gene, arMP-12 and its mutants lacking the NSm and/or 78-kDa proteins showed similar replication kinetics in interferon-competent mammalian and arthropod cells and produced similar-sized plaques in Vero E6 cells. Although the NSm and 78-kDa protein were nonessential for virus replication in cultured cells, retention of the genes coding for these proteins in RVFV strongly suggests that the NSm and 78-kDa proteins may be important for viral survival and/or establishment of infection in its hosts. Indeed, results of a competition-propagation assay suggested that RVFV expressing both NSm and the 78-kDa proteins had a selective advantage over a virus lacking both proteins in infected hosts.

Spik et al. examined the immunogenicity of two DNA vaccines, $RVFV_{+NSm}$, expressing NSm, Gn and Gc and $RVFV_{-NSm}$, expressing only Gn and Gc; immunization of mice with the former fails to elicit neutralizing antibodies and leaves the mice susceptible to wild-type RVFV challenge, whereas mice immunized with the latter produce neutralizing antibodies and are resistant to wt RVFV challenge (118). In cell culture, NSm is dispensable for RNA synthesis, RNA packaging and assembly, and any other currently known function related to the viral life cycle, leading to the speculation that NSm protein expression may suppress the induction of the humoral immune response in animal hosts. Therefore, I attempted to test whether the expression of NSm affects the production of neutralizing antibodies in infected mice. Four- to five-week old CD 1 female mice were mock-infected with a saline diluent (Hanks' balanced salt solution: HBSS) and independently infected with $10^5$ pfu of arMP-12, or $10^5$ pfu of arMP-12-del21/384. Subsequently, sera, livers, spleens, and brains were collected at 0, 2, 4, 6, 8, 10 days p.i. and subject to plaque assay for virus titers (Fig. 5.1). To determine the presence and concentration of neutralizing antibodies, virus plaque reduction neutralization test 80 ($PRNT_{80}$) was performed with sera collected at 0, 2, 4, 6, 8, 10, 14, 28 days p.i. (Fig. 5.2). Since RVFV MP-12 strain is quite attenuated in animals (24, 88, 131), viremia and infectious viruses in livers were detected only at 2 days p.i., but not later days, in both arMP-12 and arMP-12-del21/384 infections (Fig. 5.1A), while viruses in spleens could be detected in both infections up to the last day (10 days p.i.) tested in this experiment (Fig. 5.1B). In any case, the titers of detectable viruses were not higher than $10^3$ pfu/g (Fig. 5.1), and no detectable viruses were observed in any brain samples of infected mice. Although the biological significance in RVFV infection is not known, its prolonged existence in spleens seems to be general feature of RVFV infection in animals

(personal communication with Dr. C. J. Peters). In $PRNT_{80}$, arMP-12-del21/384 infection showed a similar kinetics of neutralizing antibody induction as did arMP-12 or MP-12 infection (Fig. 5.2 and data not shown) suggesting that NSm expression did not suppress neutralizing antibody production in RVFV infection, inconsistent with the past DNA vaccine study (118). However, arMP-12-del21/384 could be a good candidate for a RVFV live-attenuated vaccine in that its infection can elicit neutralizing antibody as efficiently as arMP-12 or MP-12 can, and reversion of the gene deletion is very unlikely after vaccination, which can confer much more genetic safety to a live-attenuated vaccine.

A recent study on naturally occurring mutant viruses of Maguari virus (MAGV), genus *Orthobunyavirus*, in which NSm protein is encoded between the Gn and Gc proteins, showed that an intact NSm protein is not required for the replication of MAGV in cell culture (101); RVFV NSm and MAGV NSm are 115 and 174 amino acids long, respectively, and share 14.8% amino acid sequence identity. Whether RVFV NSm protein and MAGV NSm protein share the same biological functions is unclear.
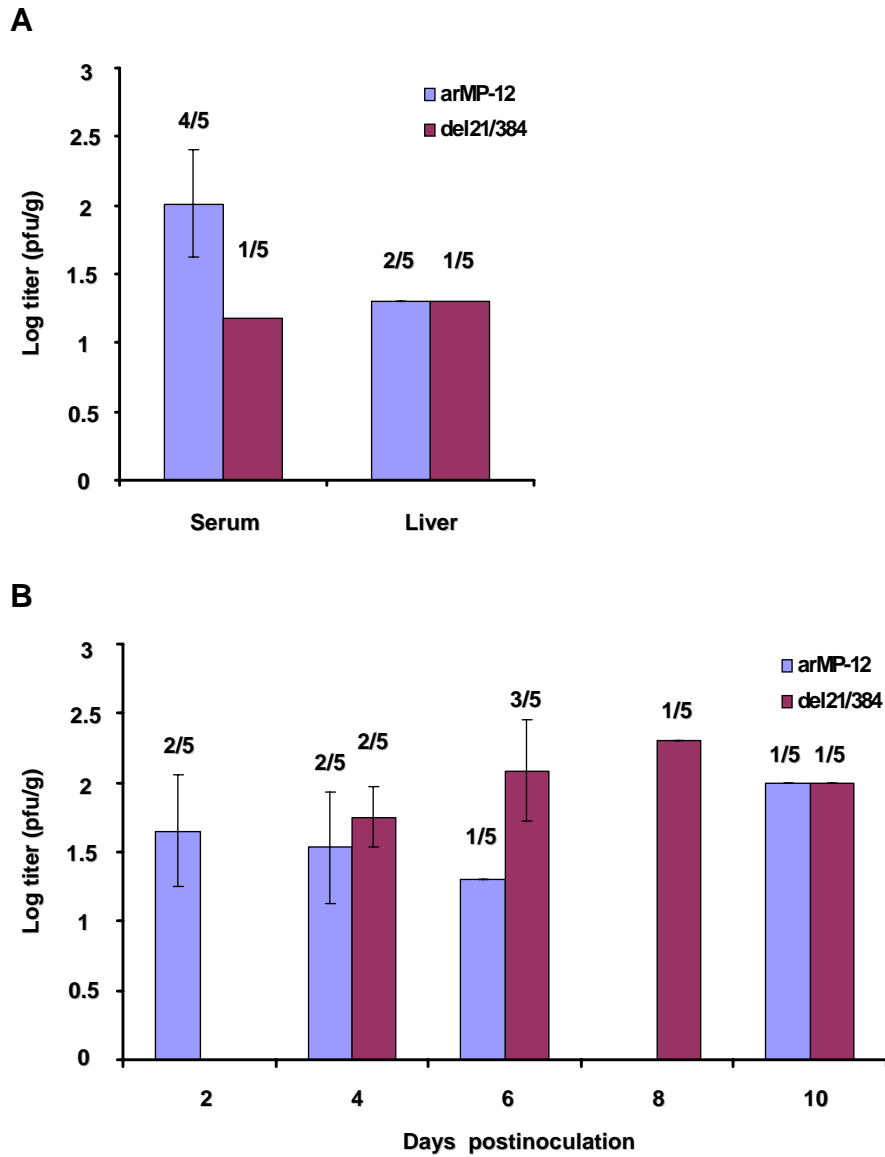
Figure 5.1: Detectable viruses in sera, livers (A), and spleens (B) in infected mice

4- to 5-week old CD 1 female mice were mock-infected with HBSS and independently infected with $10^5$ pfu of arMP-12, or arMP-12-del21/384. Sera, livers, and spleens were collected at the indicated days p.i. and titers of detectable viruses were measured by plaque assay. Five mice were used for each group per day. Number of virus-positive samples of mice was shown on the top of bars.
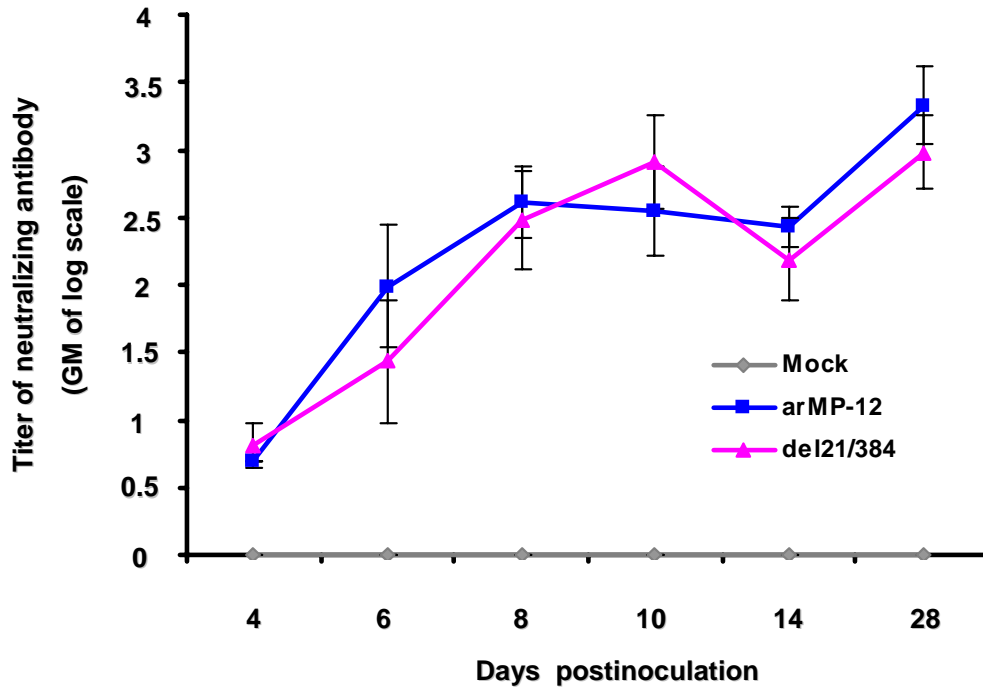
Figure 5.2: Comparison of virus plaque reduction neutralization test 80 (PRNT$_{80}$)

Four- to five-week old CD 1 female mice were mock-inoculated with HBSS and independently inoculated with $10^5$ pfu of arMP-12, or arMP-12-del21/384. Serum samples were collected from 5 to 10 mice per each group at indicated days p.i. and subject to PRNT$_{80}$. In the neutralization assay, a constant pre-determined dose (100 pfu) of MP-12 (a standard virus) was mixed with varying dilutions (1:10 to 1:10240) of test serum and incubated for 1 h at 37 °C. The mixture was then infected into Vero E6 cells in 24-well plates, followed by plaque assay. Infection of standard MP-12 (100 pfu) with normal serum was used as a standard. 80 % reduction in the number of viral plaques by the serum antibody was considered as the antibody level to be expressed as a neutralizing titer.

## III. SUPPRESSION OF VIRUS-INDUCED APOPTOSIS BY NSm PROTEIN OF RVFV

RVFV NSs protein, 78-kDa protein and NSm protein are viral accessory proteins, because they are dispensable for virus replication in cell cultures as described in Chapter 3 (55). A biological function of NSs, which suppresses host mRNA transcription, has been described (12, 78), whereas biological functions of the NSm and 78-kDa protein were unclear. By using arMP-12-del21/384, carrying a deletion in the pre-Gn region of the M gene ORF, and its parental virus, the study in Chapter 4 identified RVFV NSm protein as an inhibitor of apoptosis.

Among five in-frame AUGs in the pre-Gn region of RVFV M mRNA, the fourth AUG is mainly used for translation of Gn and Gc proteins, while the 78-KDa protein and NSm protein are translated from the first AUG and the second AUG, respectively(62, 123). In addition to these proteins, the studies in Chapters 3 and 4 showed an accumulation of a 75-kDa protein, which reacted with anti-NSm antibody, in MP-12-infected cells. Synthesis of a viral protein from the second AUG that corresponds to the 75-kDa protein was also reported in the cells expressing RVFV M segment RNA (47). I also detected an accumulation of a 73-kDa protein, which also reacted with anti-NSm antibody, in the cells supporting replication of arMP-12-delNSm/78; synthesis of the NSm protein, 78-kDa protein and 75-kDa protein did not occur in arMP-12-delNSm/78-infected cells (Fig. 3.2 and 4.2C). Replication of the MP-12 mutant carrying a substitution mutation at the third AUG resulted in an accumulation of NSm, the 78-KDa and the 75-kDa proteins, but not of the 73-kDa protein (data not shown). These data suggested that translation of the 73-kDa protein and 75-kDa protein were initiated from the third AUG and the second AUG, respectively, and the 73-kDa protein was

accumulated when the first AUG and/or second AUG were abolished. Among those proteins carrying the pre-Gn region, the NSm and the 73-kDa proteins, but not the 78-kDa protein, suppressed caspase-3 cleavage and activation in the trans-complementation experiments (Fig. 4.8). Consistent with these data, the kinetics of cell viability were similar between arMP-12-infected cells and in the cells that were infected with arMP-12-delNSm/78, which expressed 73-kDa protein, but not the 78-kDa, the 75-kDa and NSm proteins (Fig. 4.4). These data revealed that the NSm and the 73-kDa proteins, but not the 78-kDa protein, had an anti-apoptosis function. Furthermore, the data suggested that the low abundance of the 73-kDa protein could exert the anti-apoptotic activity (see Figs.4.2 and 4.8). Then, why did the 78-kDa protein, which includes the sequences that are present in NSm and the 73-kDa protein, not also exert an anti-apoptotic function? It is tempting to speculate that the 78-kDa protein translocates into the lumen of endoplasmic reticulum through its N-terminal signal peptide, whereas the NSm, 75-kDa and 73-kDa proteins lack an N-terminal signal peptide, and hence, the portion of these proteins encoded by the pre-Gn region are probably localized within the cytoplasm (46, 47, 61). If the NSm or 73-kDa proteins exert their anti-apoptotic activities in the cytoplasm, then it is not surprising that the 78-kDa protein could not exert an anti-apoptotic function, as its Pre-Gn region may be located within the lumen.

It is described that arMP-12 and its three different mutant viruses, one lacking NSm protein expression, the second lacking 78-kDa protein expression, and the third lacking the expression of both NSm and 78-kDa proteins, produce the same sizes and morphologies of plaques in Chapter 3. Because accumulation of 73-kDa protein and/or 75-kDa protein occurs in the cells infected with these mutant viruses, I suspect that expression of 73-kDa and/or 75-kDa proteins in the cells infected with these mutant

85

viruses exerted anti-apoptotic activities and contributed to the formation of plaques that are indistinguishable from those produced by arMP-12. Gerrard et al. reported the generation of ZH501 strain of RVFV lacking most of the pre-Gn region (45). Like arMP-12-del21/384, this mutant virus most probably does not express any viral proteins carrying pre-Gn region, and yet they reported that the sizes and morphologies of plaques made by this mutant virus are the same as its parental wt RVFV. It should be noted that 0.6% tragacanth gum was used as an overlay in the plaque assay in the study of Chapter 4, while Gerrard et al. used 1% agarose for the overlay. It is possible that the tragacanth gum overlay was more sensitive for detecting minute differences in plaque sizes and morphologies of RVFV.

There are ample examples that apoptotic cell death occurs in virus infection; apoptosis is induced by host immune responses, viral encoded proapoptotic proteins, or double-stranded RNA-mediated host cell responses (6, 57, 105). Induction of apoptosis after virus infection is considered to be one of the host defense mechanisms eliminating infected cells to limit viral replication and spread. Several bunyaviruses induce apoptosis in cell cultures and in vivo (18, 30, 33, 80). To secure efficient progeny virus production, viruses have developed various strategies to suppress apoptosis by expressing viral anti-apoptotic proteins (105, 112). The virus-mediated inhibition of apoptosis also contributes to the establishment of latent infections or viral oncogenesis. Large DNA viruses displaying low levels of cytotoxicity, including adenoviruses, papovaviruses, herpesviruses, poxviruses, and baculoviruses (23, 44, 105, 112, 117, 126) have been shown to carry more than one anti-apoptotic gene. In contrast to large DNA viruses, studies of anti-apoptotic proteins in RNA viruses are rather limited; several past studies suggested the presence of anti-apoptotic proteins in several picornaviruses (22), hepatitis

C virus (107), respiratory syncytial virus (RSV) (16), bunyamwera virus (67) and influenza A virus (35). RVFV NSm protein is the first viral protein in phleboviruses that showed an anti-apoptosis function. Further studies are required to assess whether other bunyaviruses also encode proteins with anti-apoptotic functions.

The number of dead cells in arMP-12-del21/384-infected cells was substantially higher than in arMP-12-infected cells after 48 h p.i. (Fig. 4.4), while both viruses showed similar virus growth kinetics (Fig. 4.3). Because efficient progeny RVFV release occurs within the first 24 h p.i. after infection at an MOI of 1 or higher in cell cultures (Fig. 4.3) (55), the majority of progeny viruses would be released prior to virus-induced apoptosis. Rapid virus replication prior to induction of apoptotic cell death is one of the strategies that some RNA viruses have employed to secure efficient progeny production (68, 72), and it appears that RVFV also uses this strategy to circumvent the negative effects of virus-induced apoptosis for virus production. If RVFV always replicates quickly prior to execution of apoptotic cell death, then why is the pre-Gn region in the RVFV M segment strictly retained in all RVFV thus far sequenced (14)? A virus such as RVFV with such a rapid progression to cell death in virtually all vertebrate cell types infected might require prolongation of the time of productive infection. It is established that when cells that are undergoing transcription and/or translational suppression are exposed to tumor necrosis factor-$\alpha$, they quickly die by apoptosis (2, 122). It is also known that RVFV replication efficiently suppresses host transcription and translation {Le May, 2004 #14}. Accordingly, I suspect that a combination of virus replication and exposure of the infected cells to some extracellular factors, e.g., tumor necrosis factor-$\alpha$, may induce rapid apoptosis prior to the completion of maximum progeny virus production in RVFV-infected mammals; without NSm, RVFV may not be able to amplify efficiently in an

infected host. Consistent with this notion, a recombinant wt RVFV lacking most of the pre-Gn region has an attenuated virulence in rats (13), suggesting that proteins encoded in the pre-Gn region have some role in RVFV virulence.

The data in Chapter 4 suggested that RVFV infection triggered apoptosis mainly through caspase-8 activation, which is involved in a death receptor-mediated, extrinsic, apoptotic pathway, and that NSm expression suppressed caspase-8 activation (Fig. 4.7). It is also observed that NSm efficiently inhibited STP-induced caspase-8 and caspase-9 activities (Fig. 4.9). Because it is well established that activated caspase-8 can activate caspase-9 by provoking the release of cytochrome c from mitochondria via the cleavage of Bid (79, 84), it is conceivable that the NSm protein inhibited either activated caspase-8 activity or an apoptotic pathway that activates caspase-8, resulting in the suppression of caspase-9 activation as well. However, I cannot exclude the possibility that the NSm protein also directly inhibits the activation of downstream caspases, including caspase-9 and caspase-3.

In summary, my dissertation demonstrates the development of a reverse genetics system for RVFV, which is the first for any phleboviruses. Characterization of recombinant mutant viruses showed that NSm and 78-kDa proteins of RVFV were dispensable for virus to replicate efficiently in cell culture systems, and that NSm protein suppressed virus-induced apoptosis via inhibition of caspase activation. The findings described in this dissertation raise several questions about the mechanism of apoptosis inhibition by NSm and the biological significance of apoptosis inhibition in RVFV pathogenesis. Answers to these questions would significantly contribute towards our understanding of the role of NSm protein in the life cycle of RVFV.

# References

1.  **Büchen-Osmond, C.** (Ed), (2006) Index to ICTVdB virus descriptions. In: ICTVdB - The Universal Virus Database, version 4. ICTVdB Management, Mailman School of Public Health, Columbia University, New York, NY, USA

2.  **Aggarwal, B. B., W. J. Kohr, P. E. Hass, B. Moffat, S. A. Spencer, W. J. Henzel, T. S. Bringman, G. E. Nedwin, D. V. Goeddel, and R. N. Harkins.** 1985. Human tumor necrosis factor. Production, purification, and characterization. J Biol Chem **260:**2345-2354.

3.  **Anderson, G. W., Jr., T. W. Slone, Jr., and C. J. Peters.** 1987. Pathogenesis of Rift Valley fever virus (RVFV) in inbred rats. Microb Pathog **2:**283-293.

4.  **Anderson, G. W., Jr., and J. F. Smith.** 1987. Immunoelectron microscopy of Rift Valley fever viral morphogenesis in primary rat hepatocytes. Virology **161:**91-100.

5.  **Arikawa, J., A. L. Schmaljohn, J. M. Dalrymple, and C. S. Schmaljohn.** 1989. Characterization of Hantaan virus envelope glycoprotein antigenic determinants defined by monoclonal antibodies. J Gen Virol **70 ( Pt 3):**615-624.

6.  **Balachandran, S., C. N. Kim, W. C. Yeh, T. W. Mak, K. Bhalla, and G. N. Barber.** 1998. Activation of the dsRNA-dependent protein kinase, PKR, induces apoptosis through FADD-mediated death signaling. Embo J **17:**6888-6902.

7.  **Balkhy, H. H., and Z. A. Memish.** 2003. Rift Valley fever: an uninvited zoonosis in the Arabian peninsula. Int J Antimicrob Agents **21:**153-157.

8.  **Banerjee, S., K. Narayanan, T. Mizutani, and S. Makino.** 2002. Murine coronavirus replication-induced p38 mitogen-activated protein kinase activation promotes interleukin-6 production and virus replication in cultured cells. J Virol **76:**5937-5948.

9.     **Barber, G. N.** 2001. Host defense, viruses and apoptosis. Cell Death Differ **8:**113-126.

10.     **Barral, P. M., J. M. Morrison, J. Drahos, P. Gupta, D. Sarkar, P. B. Fisher, and V. R. Racaniello.** 2007. MDA-5 is cleaved in poliovirus-infected cells. J Virol **81:**3677-3684.

11.     **Bertin, J., R. C. Armstrong, S. Ottilie, D. A. Martin, Y. Wang, S. Banks, G. H. Wang, T. G. Senkevich, E. S. Alnemri, B. Moss, M. J. Lenardo, K. J. Tomaselli, and J. I. Cohen.** 1997. Death effector domain-containing herpesvirus and poxvirus proteins inhibit both Fas- and TNFR1-induced apoptosis. Proc Natl Acad Sci U S A **94:**1172-1176.

12.     **Billecocq, A., M. Spiegel, P. Vialat, A. Kohl, F. Weber, M. Bouloy, and O. Haller.** 2004. NSs protein of Rift Valley fever virus blocks interferon production by inhibiting host gene transcription. J Virol **78:**9798-9806.

13.     **Bird, B. H., C. G. Albarino, and S. T. Nichol.** 2007. Rift Valley fever virus lacking NSm proteins retains high virulence in vivo and may provide a model of human delayed onset neurologic disease. Virology **362:**10-15.

14.     **Bird, B. H., M. L. Khristova, P. E. Rollin, T. G. Ksiazek, and S. T. Nichol.** 2007. Complete genome analysis of 33 ecologically and biologically diverse Rift Valley fever virus strains reveals widespread virus movement and low genetic diversity due to recent common ancestry. J Virol **81:**2805-2816.

15.     **Bishop, D. H., K. G. Gould, H. Akashi, and C. M. Clerx-van Haaster.** 1982. The complete sequence and coding content of snowshoe hare bunyavirus small (S) viral RNA species. Nucleic Acids Res **10:**3703-3713.

16.     **Bitko, V., O. Shulyayeva, B. Mazumder, A. Musiyenko, M. Ramaswamy, D. C. Look, and S. Barik.** 2007. Nonstructural proteins of respiratory syncytial virus suppress premature apoptosis by an NF-kappaB-dependent, interferon-independent mechanism and facilitate virus growth. J Virol **81:**1786-1795.

17.  **Blakqori, G., G. Kochs, O. Haller, and F. Weber.** 2003. Functional L polymerase of La Crosse virus allows in vivo reconstitution of recombinant nucleocapsids. J Gen Virol **84:**1207-1214.

18.  **Blakqori, G., and F. Weber.** 2005. Efficient cDNA-based rescue of La Crosse bunyaviruses expressing or lacking the nonstructural protein NSs. J Virol **79:**10420-10428.

19.  **Boatright, K. M., and G. S. Salvesen.** 2003. Mechanisms of caspase activation. Curr Opin Cell Biol **15:**725-731.

20.  **Bouloy, M., C. Janzen, P. Vialat, H. Khun, J. Pavlovic, M. Huerre, and O. Haller.** 2001. Genetic evidence for an interferon-antagonistic function of rift valley fever virus nonstructural protein NSs. J Virol **75:**1371-1377.

21.  **Bridgen, A., and R. M. Elliott.** 1996. Rescue of a segmented negative-strand RNA virus entirely from cloned complementary DNAs. Proc Natl Acad Sci U S A **93:**15400-15404.

22.  **Buenz, E. J., and C. L. Howe.** 2006. Picornaviruses and cell death. Trends Microbiol **14:**28-36.

23.  **Callus, B. A., and D. L. Vaux.** 2007. Caspase inhibitors: viral, cellular and chemical. Cell Death Differ **14:**73-78.

24.  **Caplen, H., C. J. Peters, and D. H. Bishop.** 1985. Mutagen-directed attenuation of Rift Valley fever virus as a method for vaccine development. J Gen Virol **66:**2271-2277.

25.  **CDC.** 2007. Rift Valley Fever Outbreak---Kenya, November 2006---January 2007, MMWR **56:**73-76.

26.  **Clem, R. J., M. Fechheimer, and L. K. Miller.** 1991. Prevention of apoptosis by a baculovirus gene during infection of insect cells. Science **254:**1388-1390.

27.    **Clem, R. J., and L. K. Miller.** 1993. Apoptosis reduces both the in vitro replication and the in vivo infectivity of a baculovirus. J Virol **67:**3730-3738.

28.    **Coetzer, J. A.** 1982. The pathology of Rift Valley fever. II. Lesions occurring in field cases in adult cattle, calves and aborted foetuses. Onderstepoort J Vet Res **49:**11-17.

29.    **Cohen, J. J., R. C. Duke, V. A. Fadok, and K. S. Sellins.** 1992. Apoptosis and programmed cell death in immunity. Annu Rev Immunol **10:**267-293.

30.    **Colon-Ramos, D. A., P. M. Irusta, E. C. Gan, M. R. Olson, J. Song, R. I. Morimoto, R. M. Elliott, M. Lombard, R. Hollingsworth, J. M. Hardwick, G. K. Smith, and S. Kornbluth.** 2003. Inhibition of translation and induction of apoptosis by Bunyaviral nonstructural proteins bearing sequence similarity to reaper. Mol Biol Cell **14:**4162-4172.

31.    **Conzelmann, K. K.** 2004. Reverse genetics of mononegavirales. Curr Top Microbiol Immunol **283:**1-41.

32.    **Diaz, M. O., S. Ziemin, M. M. Le Beau, P. Pitha, S. D. Smith, R. R. Chilcote, and J. D. Rowley.** 1988. Homozygous deletion of the alpha- and beta 1-interferon genes in human leukemia and derived cell lines. Proc Natl Acad Sci U S A **85:**5259-5263.

33.    **Ding, X., F. Xu, H. Chen, R. B. Tesh, and S. Y. Xiao.** 2005. Apoptosis of hepatocytes caused by Punta Toro virus (Bunyaviridae: Phlebovirus) and its implication for Phlebovirus pathogenesis. Am J Pathol **167:**1043-1049.

34.    **Dunn, E. F., D. C. Pritlove, H. Jin, and R. M. Elliott.** 1995. Transcription of a recombinant bunyavirus RNA template by transiently expressed bunyavirus proteins. Virology **211:**133-143.

35.    **Ehrhardt, C., T. Wolff, S. Pleschka, O. Planz, W. Beermann, J. G. Bode, M. Schmolke, and S. Ludwig.** 2007. Influenza A virus NS1 protein activates the PI3K/Akt pathway to mediate antiapoptotic signaling responses. J Virol **81:**3058-3067.

36. **Ellis, D. S., P. V. Shirodaria, E. Fleming, and D. I. Simpson.** 1988. Morphology and development of Rift Valley fever virus in Vero cell cultures. J Med Virol **24:**161-174.

37. **Everett, H., and G. McFadden.** 1999. Apoptosis: an innate immune response to virus infection. Trends Microbiol **7:**160-165.

38. **Fenner, R.** 1975. The classification and nomenclature of viruses. Intervirology **6:**1-12.

39. **Flick, K., J. W. Hooper, C. S. Schmaljohn, R. F. Pettersson, H. Feldmann, and R. Flick.** 2003. Rescue of Hantaan virus minigenomes. Virology **306:**219-224.

40. **Flick, R., and M. Bouloy.** 2005. Rift Valley fever virus. Curr Mol Med **5:**827-834.

41. **Flick, R., K. Flick, H. Feldmann, and F. Elgh.** 2003. Reverse genetics for crimean-congo hemorrhagic fever virus. J Virol **77:**5997-6006.

42. **Flick, R., and R. F. Pettersson.** 2001. Reverse genetics system for Uukuniemi virus (Bunyaviridae): RNA polymerase I-catalyzed expression of chimeric viral RNAs. J Virol **75:**1643-1655.

43. **Gargan, T. P., 2nd, G. G. Clark, D. J. Dohm, M. J. Turell, and C. L. Bailey.** 1988. Vector potential of selected North American mosquito species for Rift Valley fever virus. Am J Trop Med Hyg **38:**440-446.

44. **Garnett, T. O., M. Filippova, and P. J. Duerksen-Hughes.** 2006. Accelerated degradation of FADD and procaspase 8 in cells expressing human papilloma virus 16 E6 impairs TRAIL-mediated apoptosis. Cell Death Differ **13:**1915-1926.

45. **Gerrard, S. R., B. H. Bird, C. G. Albarino, and S. T. Nichol.** 2007. The NSm proteins of Rift Valley fever virus are dispensable for maturation, replication and infection. Virology **359:**459-465.

46.  **Gerrard, S. R., and S. T. Nichol.** 2002. Characterization of the Golgi retention motif of Rift Valley fever virus G(N) glycoprotein. J Virol **76:**12200-12210.

47.  **Gerrard, S. R., and S. T. Nichol.** 2007. Synthesis, proteolytic processing and complex formation of N-terminally nested precursor proteins of the Rift Valley fever virus glycoproteins. Virology **357:**124-133.

48.  **Gerrard, S. R., P. E. Rollin, and S. T. Nichol.** 2002. Bidirectional infection and release of Rift Valley fever virus in polarized epithelial cells. Virology **301:**226-235.

49.  **Goldsmith, C. S., L. H. Elliott, C. J. Peters, and S. R. Zaki.** 1995. Ultrastructural characteristics of Sin Nombre virus, causative agent of hantavirus pulmonary syndrome. Arch Virol **140:**2107-2122.

50.  **Han, Z., P. Pantazis, T. S. Lange, J. H. Wyche, and E. A. Hendrickson.** 2000. The staurosporine analog, Ro-31-8220, induces apoptosis independently of its ability to inhibit protein kinase C. Cell Death Differ **7:**521-530.

51.  **Harada, K., Y. Sato, K. Itatsu, K. Isse, H. Ikeda, M. Yasoshima, Y. Zen, A. Matsui, and Y. Nakanuma.** 2007. Innate immune response to double-stranded RNA in biliary epithelial cells is associated with the pathogenesis of biliary atresia. Hepatology **46:**1146-1154.

52.  **Hewlett, M. J., R. F. Pettersson, and D. Baltimore.** 1977. Circular forms of Uukuniemi virion RNA: an electron microscopic study. J Virol **21:**1085-1093.

53.  **Hu, F. Q., C. A. Smith, and D. J. Pickup.** 1994. Cowpox virus contains two copies of an early gene encoding a soluble secreted form of the type II TNF receptor. Virology **204:**343-356.

54.  **Ikegami, T., C. J. Peters, and S. Makino.** 2005. Rift valley fever virus nonstructural protein NSs promotes viral RNA replication and transcription in a minigenome system. J Virol **79:**5606-5615.

55.	**Ikegami, T., S. Won, C. J. Peters, and S. Makino.** 2006. Rescue of Infectious Rift Valley Fever Virus Entirely from cDNA, Analysis of Virus Lacking the NSs Gene, and Expression of a Foreign Gene. J Virol **80:**2933-2940.

56.	**Ikegami, T., S. Won, C. J. Peters, and S. Makino.** 2005. Rift Valley fever virus NSs mRNA is transcribed from an incoming anti-viral-sense S RNA segment. J Virol **79:**12106-12111.

57.	**Iordanov, M. S., J. D. Kirsch, O. P. Ryabinina, J. Wong, P. N. Spitz, V. B. Korcheva, A. Thorburn, and B. E. Magun.** 2005. Recruitment of TRADD, FADD, and caspase 8 to double-stranded RNA-triggered death inducing signaling complexes (dsRNA-DISCs). Apoptosis **10:**167-176.

58.	**Ito, N., M. Takayama-Ito, K. Yamada, J. Hosokawa, M. Sugiyama, and N. Minamoto.** 2003. Improved recovery of rabies virus from cloned cDNA using a vaccinia virus-free reverse genetics system. Microbiol Immunol **47:**613-617.

59.	**Jin, H., and R. M. Elliott.** 1993. Characterization of Bunyamwera virus S RNA that is transcribed and replicated by the L protein expressed from recombinant vaccinia virus. J Virol **67:**1396-1404.

60.	**Jin, H., and R. M. Elliott.** 1991. Expression of functional Bunyamwera virus L protein by recombinant vaccinia viruses. J Virol **65:**4182-4189.

61.	**Kakach, L. T., J. A. Suzich, and M. S. Collett.** 1989. Rift Valley fever virus M segment: phlebovirus expression strategy and protein glycosylation. Virology **170:**505-510.

62.	**Kakach, L. T., T. L. Wasmoen, and M. S. Collett.** 1988. Rift Valley fever virus M segment: use of recombinant vaccinia viruses to study Phlebovirus gene expression. J Virol **62:**826-833.

63.	**Kamitani, W., K. Narayanan, C. Huang, K. Lokugamage, T. Ikegami, N. Ito, H. Kubo, and S. Makino.** 2006. Severe acute respiratory syndrome coronavirus nsp1 protein suppresses host gene expression by promoting host mRNA degradation. Proc Natl Acad Sci U S A **103:**12885-12890.

64. **Keegan, K., M. S. Collett.** 1986. Use of bacterial expression cloning to define the amino acid sequences of antigenic determinants on the G2 glycoprotein of Rift Valley fever virus. J Virol **58:**263-270.

65. **Kerr, J. F., A. H. Wyllie, and A. R. Currie.** 1972. Apoptosis: a basic biological phenomenon with wide-ranging implications in tissue kinetics. Br J Cancer **26:**239-257.

66. **Kikkert, M., J. Van Lent, M. Storms, P. Bodegom, R. Kormelink, and R. Goldbach.** 1999. Tomato spotted wilt virus particle morphogenesis in plant cells. J Virol **73:**2288-2297.

67. **Kohl, A., R. F. Clayton, F. Weber, A. Bridgen, R. E. Randall, and R. M. Elliott.** 2003. Bunyamwera virus nonstructural protein NSs counteracts interferon regulatory factor 3-mediated induction of early cell death. J Virol **77:**7999-8008.

68. **Kopecky, S. A., M. C. Willingham, and D. S. Lyles.** 2001. Matrix protein and another viral component contribute to induction of apoptosis in cells infected with vesicular stomatitis virus. J Virol **75:**12169-12181.

69. **Kormelink, R., P. de Haan, C. Meurs, D. Peters, and R. Goldbach.** 1992. The nucleotide sequence of the M RNA segment of tomato spotted wilt virus, a bunyavirus with two ambisense RNA segments. J Gen Virol **73:**2795-2804.

70. **Kormelink, R., P. de Haan, D. Peters, and R. Goldbach.** 1992. Viral RNA synthesis in tomato spotted wilt virus-infected Nicotiana rustica plants. J Gen Virol **73:**687-693.

71. **Koyama, A. H.** 1995. Induction of apoptotic DNA fragmentation by the infection of vesicular stomatitis virus. Virus Res **37:**285-290.

72. **Koyama, A. H., A. Adachi, and H. Irie.** 2003. Physiological significance of apoptosis during animal virus infection. Int Rev Immunol **22:**341-359.

73.   **Koyama, A. H., H. Irie, T. Fukumori, S. Hata, S. Iida, H. Akari, and A. Adachi.** 1998. Role of virus-induced apoptosis in a host defense mechanism against virus infection. J Med Invest **45:**37-45.

74.   **Krohn, A. J., E. Preis, and J. H. Prehn.** 1998. Staurosporine-induced apoptosis of cultured rat hippocampal neurons involves caspase-1-like proteases as upstream initiators and increased production of superoxide as a main downstream effector. J Neurosci **18:**8186-8197.

75.   **Kumar, S.** 2007. Caspase function in programmed cell death. Cell Death Differ **14:**32-43.

76.   **Kurokawa, M., A. H. Koyama, S. Yasuoka, and A. Adachi.** 1999. Influenza virus overcomes apoptosis by rapid multiplication. Int J Mol Med **3:**527-530.

77.   **Lamkanfi, M., N. Festjens, W. Declercq, T. Vanden Berghe, and P. Vandenabeele.** 2007. Caspases in cell survival, proliferation and differentiation. Cell Death Differ **14:**44-55.

78.   **Le May, N., S. Dubaele, L. Proietti De Santis, A. Billecocq, M. Bouloy, and J. M. Egly.** 2004. TFIIH transcription factor, a target for the Rift Valley hemorrhagic fever virus. Cell **116:**541-550.

79.   **Li, H., H. Zhu, C. J. Xu, and J. Yuan.** 1998. Cleavage of BID by caspase 8 mediates the mitochondrial damage in the Fas pathway of apoptosis. Cell **94:**491-501.

80.   **Li, X. D., S. Kukkonen, O. Vapalahti, A. Plyusnin, H. Lankinen, and A. Vaheri.** 2004. Tula hantavirus infection of Vero E6 cells induces apoptosis involving caspase 8 activation. J Gen Virol **85:**3261-3268.

81.   **Linthicum, K. J., F. G. Davies, A. Kairo, and C. L. Bailey.** 1985. Rift Valley fever virus (family Bunyaviridae, genus Phlebovirus). Isolations from Diptera collected during an inter-epizootic period in Kenya. J Hyg (Lond) **95:**197-209.

82.    **Lopez, N., R. Muller, C. Prehaud, and M. Bouloy.** 1995. The L protein of Rift Valley fever virus can rescue viral ribonucleoproteins and transcribe synthetic genome-like RNA molecules. J Virol **69:**3972-3979.

83.    **Lowen, A. C., C. Noonan, A. McLees, and R. M. Elliott.** 2004. Efficient bunyavirus rescue from cloned cDNA. Virology **330:**493-500.

84.    **Luo, X., I. Budihardjo, H. Zou, C. Slaughter, and X. Wang.** 1998. Bid, a Bcl2 interacting protein, mediates cytochrome c release from mitochondria in response to activation of cell surface death receptors. Cell **94:**481-490.

85.    **Luytjes, W., M. Krystal, M. Enami, J. D. Parvin, and P. Palese.** 1989. Amplification, expression, and packaging of foreign gene by influenza virus. Cell **59:**1107-1113.

86.    **Martin, S. J., C. P. Reutelingsperger, A. J. McGahon, J. A. Rader, R. C. van Schie, D. M. LaFace, and D. R. Green.** 1995. Early redistribution of plasma membrane phosphatidylserine is a general feature of apoptosis regardless of the initiating stimulus: inhibition by overexpression of Bcl-2 and Abl. J Exp Med **182:**1545-1556.

87.    **Meegan, J. M., G. M. Khalil, H. Hoogstraal, and F. K. Adham.** 1980. Experimental transmission and field isolation studies implicating Culex pipiens as a vector of Rift Valley fever virus in Egypt. Am J Trop Med Hyg **29:**1405-1410.

88.    **Morrill, J. C., and C. J. Peters.** 2003. Pathogenicity and neurovirulence of a mutagen-attenuated Rift Valley fever vaccine in rhesus monkeys. Vaccine **21:**2994-3002.

89.    **Mosca, J. D., and P. M. Pitha.** 1986. Transcriptional and posttranscriptional regulation of exogenous human beta interferon gene in simian cells defective in interferon synthesis. Mol Cell Biol **6:**2279-2283.

90.    **Neumann, G., M. A. Whitt, and Y. Kawaoka.** 2002. A decade after the generation of a negative-sense RNA virus from cloned cDNA - what have we learned? J Gen Virol **83:**2635-2662.

91.  **Pattnaik, A. K., L. A. Ball, A. W. LeGrone, and G. W. Wertz.** 1992. Infectious defective interfering particles of VSV from transcripts of a cDNA clone. Cell **69:**1011-1020.

92.  **Peters, C. J.** 2000. Are hemorrhagic fever viruses practical agents for biological terrorism?, p. 203-211. *In* W. M. Scheld, W. A. Craig, and J. M. Hughes (ed.), Emerging infections, vol. 4. ASM press, Wahington, D. .C.

93.  **Peters, C. J.** 1997. Emergence of Rift Valley fever, p. 253-264. *In* J. F. Saluzzo, B. Dodet (ed.), Factors in the emergence of arbovirus diseases. Elsevier, Paris, France.

94.  **Peters, C. J., and J. W. LeDuc.** 1991. Bunyaviridae: bunyaviruses, phleboviruses and related viruses, p. 571-614. *In* R. B. Belshe (ed.), Textbook of human virology, 2nd ed. Mosby Year Book, St. Louis, Mo.

95.  **Peters, C. J., D. Jones, R. Trotter, J. Donaldson, J. White, E. Stephen, and T. W. Slone, Jr.** 1988. Experimental Rift Valley fever in rhesus macaques. Arch Virol **99:**31-44.

96.  **Peters, C. J., and J. W. LeDuc.** 1999. Bunyaviridae: Bunyaviruses, Phleboviruses, and related viruses, 2nd ed. Mosby Year Book.

97.  **Peters, C. J., and J. M. Meegan.** 1989. Rift Valley fever. CRC Press, Boca Raton, Fla.

98.  **Pifat, D. Y., M. C. Osterling, and J. F. Smith.** 1988. Antigenic analysis of Punta Toro virus and identification of protective determinants with monoclonal antibodies. Virology **167:**442-450.

99.  **Pilder, S., J. Logan, and T. Shenk.** 1984. Deletion of the gene encoding the adenovirus 5 early region 1b 21,000-molecular-weight polypeptide leads to degradation of viral and host cell DNA. J Virol **52:**664-671.

100. **Pittman, P. R., C. T. Liu, T. L. Cannon, R. S. Makuch, J. A. Mangiafico, P. H. Gibbs, and C. J. Peters.** 1999. Immunogenicity of an inactivated Rift Valley fever vaccine in humans: a 12-year experience. Vaccine **18:**181-189.

101. **Pollitt, E., J. Zhao, P. Muscat, and R. M. Elliott.** 2006. Characterization of Maguari orthobunyavirus mutants suggests the nonstructural protein NSm is not essential for growth in tissue culture. Virology **348:**224-232.

102. **Prehaud, C., N. Lopez, M. J. Blok, V. Obry, and M. Bouloy.** 1997. Analysis of the 3' terminal sequence recognized by the Rift Valley fever virus transcription complex in its ambisense S segment. Virology **227:**189-197.

103. **Racaniello, V. R., and D. Baltimore.** 1981. Cloned poliovirus complementary DNA is infectious in mammalian cells. Science **214:**916-919.

104. **Ravkov, E. V., S. T. Nichol, and R. W. Compans.** 1997. Polarized entry and release in epithelial cells of Black Creek Canal virus, a New World hantavirus. J Virol **71:**1147-1154.

105. **Roulston, A., R. C. Marcellus, and P. E. Branton.** 1999. Viruses and apoptosis. Annu Rev Microbiol **53:**577-628.

106. **Ruggli, N., and C. M. Rice.** 1999. Functional cDNA clones of the Flaviviridae: strategies and applications. Adv Virus Res **53:**183-207.

107. **Saito, K., K. Meyer, R. Warner, A. Basu, R. B. Ray, and R. Ray.** 2006. Hepatitis C virus core protein inhibits tumor necrosis factor alpha-mediated apoptosis by a protective effect involving cellular FLICE inhibitory protein. J Virol **80:**4372-4379.

108. **Schmaljohn, C. a. J. W. H.** 2001. Bunyaviridae: the viruses and their replication, p. 1581-1602, 4th ed. Lippincott, Williams & Wilkins, Philadelphia, PA.

109. **Schmaljohn, C. S., and S.T. Nichol.** 2007. Bunyaviruses, p. 1741-1789. *In* B. N. Fields, Knipe, D.M.,Howley, P.M., Griffin, D.E. (ed.), Fields Virology, vol. 2. Lippincott Williams and Wilkins, Philadelphia.

110. **Schmaljohn, C. S., M. D. Parker, W. H. Ennis, J. M. Dalrymple, M. S. Collett, J. A. Suzich, and A. L. Schmaljohn.** 1989. Baculovirus expression of the M genome segment of Rift Valley fever virus and examination of antigenic and immunogenic properties of the expressed proteins. Virology **170:**184-192.

111. **Schnell, M. J., T. Mebatsion, and K. K. Conzelmann.** 1994. Infectious rabies viruses from cloned cDNA. Embo J **13:**4195-4203.

112. **Shen, Y., and T. E. Shenk.** 1995. Viruses and apoptosis. Curr Opin Genet Dev **5:**105-111.

113. **Shoemaker, T., C. Boulianne, M. J. Vincent, L. Pezzanite, M. M. Al-Qahtani, Y. Al-Mazrou, A. S. Khan, P. E. Rollin, R. Swanepoel, T. G. Ksiazek, and S. T. Nichol.** 2002. Genetic analysis of viruses associated with emergence of Rift Valley fever in Saudi Arabia and Yemen, 2000-01. Emerg Infect Dis **8:**1415-1420.

114. **Siam, A. L., and J. M. Meegan.** 1980. Ocular disease resulting from infection with Rift Valley fever virus. Trans R Soc Trop Med Hyg **74:**539-541.

115. **Siam, A. L., J. M. Meegan, and K. F. Gharbawi.** 1980. Rift Valley fever ocular manifestations: observations during the 1977 epidemic in Egypt. Br J Ophthalmol **64:**366-374.

116. **Simons, J. F., U. Hellman, and R. F. Pettersson.** 1990. Uukuniemi virus S RNA segment: ambisense coding strategy, packaging of complementary strands into virions, and homology to members of the genus Phlebovirus. J Virol **64:**247-255.

117. **Skaletskaya, A., L. M. Bartle, T. Chittenden, A. L. McCormick, E. S. Mocarski, and V. S. Goldmacher.** 2001. A cytomegalovirus-encoded inhibitor of apoptosis that suppresses caspase-8 activation. Proc Natl Acad Sci U S A **98:**7829-7834.

118. **Spik, K., A. Shurtleff, A. K. McElroy, M. C. Guttieri, J. W. Hooper, and C. Schmaljohn.** 2005. Immunogenicity of combination DNA vaccines for Rift Valley fever virus, tick-borne encephalitis virus, Hantaan virus, and Crimean Congo hemorrhagic fever virus. Vaccine **24:** 4657-4666.

119. **Stepczynska, A., K. Lauber, I. H. Engels, O. Janssen, D. Kabelitz, S. Wesselborg, and K. Schulze-Osthoff.** 2001. Staurosporine and conventional anticancer drugs induce overlapping, yet distinct pathways of apoptosis and caspase activation. Oncogene **20:**1193-1202.

120. **Storms, M. M., R. Kormelink, D. Peters, J. W. Van Lent, and R. W. Goldbach.** 1995. The nonstructural NSm protein of tomato spotted wilt virus induces tubular structures in plant and insect cells. Virology **214:**485-493.

121. **Struthers, J. K., R. Swanepoel, and S. P. Shepherd.** 1984. Protein synthesis in Rift Valley fever virus-infected cells. Virology **134:**118-124.

122. **Sugarman, B. J., B. B. Aggarwal, P. E. Hass, I. S. Figari, M. A. Palladino, Jr., and H. M. Shepard.** 1985. Recombinant human tumor necrosis factor-alpha: effects on proliferation of normal and transformed cells in vitro. Science **230:**943-945.

123. **Suzich, J. A., and M. S. Collett.** 1988. Rift Valley fever virus M segment: cell-free transcription and translation of virus-complementary RNA. Virology **164:**478-486.

124. **Suzich, J. A., L. T. Kakach, and M. S. Collett.** 1990. Expression strategy of a phlebovirus: biogenesis of proteins from the Rift Valley fever virus M segment. J Virol **64:**1549-1555.

125. **Thompson, C. B.** 1995. Apoptosis in the pathogenesis and treatment of disease. Science **267:**1456-1462.

126. **Tschopp, J., M. Thome, K. Hofmann, and E. Meinl.** 1998. The fight of viruses against apoptosis. Curr Opin Genet Dev **8:**82-87.

127. **Turell, M. J., M. E. Faran, M. Cornet, and C. L. Bailey.** 1988. Vector competence of Senegalese Aedes fowleri (Diptera: Culicidae) for Rift Valley fever virus. J Med Entomol **25:**262-266.

128. **Turell, M. J., and B. H. Kay.** 1998. Susceptibility of selected strains of Australian mosquitoes (Diptera: Culicidae) to Rift Valley fever virus. J Med Entomol **35:**132-135.

129. **Urquidi, V., and D. H. Bishop.** 1992. Non-random reassortment between the tripartite RNA genomes of La Crosse and snowshoe hare viruses. J Gen Virol **73 ( Pt 9):**2255-2265.

130. **Vermes, I., C. Haanen, H. Steffens-Nakken, and C. Reutelingsperger.** 1995. A novel assay for apoptosis. Flow cytometric detection of phosphatidylserine expression on early apoptotic cells using fluorescein labelled Annexin V. J Immunol Methods **184:**39-51.

131. **Vialat, P., R. Muller, T. H. Vu, C. Prehaud, and M. Bouloy.** 1997. Mapping of the mutations present in the genome of the Rift Valley fever virus attenuated MP12 strain and their putative role in attenuation. Virus Res **52:**43-50.

132. **Weber, F., E. F. Dunn, A. Bridgen, and R. M. Elliott.** 2001. The Bunyamwera virus nonstructural protein NSs inhibits viral RNA synthesis in a minireplicon system. Virology **281:**67-74.

133. **Won, S., T. Ikegami, C. J. Peters, and S. Makino.** 2006. NSm and 78-kilodalton proteins of Rift Valley fever virus are nonessential for viral replication in cell culture. J Virol **80:**8274-8278.

134. **Woods, C. W., A. M. Karpati, T. Grein, N. McCarthy, P. Gaturuku, E. Muchiri, L. Dunster, A. Henderson, A. S. Khan, R. Swanepoel, I. Bonmarin, L. Martin, P. Mann, B. L. Smoak, M. Ryan, T. G. Ksiazek, R. R. Arthur, A. Ndikuyeze, N. N. Agata, and C. J. Peters.** 2002. An outbreak of Rift Valley fever in Northeastern Kenya, 1997-98. Emerg Infect Dis **8:**138-144.

135. **Zeller, H. G., D. Fontenille, M. Traore-Lamizana, Y. Thiongane, and J. P. Digoutte.** 1997. Enzootic activity of Rift Valley fever virus in Senegal. Am J Trop Med Hyg **56:**265-272.

# VITA


Sungyong Won


Sungyong Won was born in Seoul, Republic of Korea on August 27, 1971 to Yongok Won and Youngsoon Kim. He is married to Jungsuk Lee and has two children, Jonghyun and Jongbin. Sungyong majored in Biology and received his Bachelor of Science degree from Kyung Hee University in Korea. During his undergraduate studies, Sungyong became interested in virology and continued his scientific training at the Graduate School of Kyung Hee University. While at Kyung Hee University, Sungyong conducted research related to the molecular virology of Japanese encephalitis virus, and received his Master of Science degree in the area of microbiology. Sungyong continued his virology training at the University of Texas Medical Branch (UTMB) under the supervision of Dr. Shinji Makino and Dr. C. J. Peters and was involved in studies of Rift Valley fever virus. His dissertation demonstrates the establishment of reverse genetics system of Rift Valley fever virus and addresses questions about functions of its nonstructural proteins.

During his graduate study at UTMB, Sungyong has been awarded a number of competitive awards. He has held a pre-doctoral fellowship sponsored by the McLaughlin Fund from 2006 to 2007. He was also the recipient of a scholarship (2006, Curtis W. Lambert Scholarship) from UTMB Graduate School of Biomedical Sciences, and travel awards (2006, 2007, Annual Meeting Travel Award from the American society for virology; 2007, University Network Summit on Research and Education Travel Award from the U.S. Department of Homeland Security; 2007, National Graduate Student Research Festival Travel Award from the National Institutes of Health).

## Education

B.S., February 1999, Kyung Hee University, Seoul, Korea
M.S., February 2001, Kyung Hee University, Seoul, Korea

## Teaching Experience

2001-2003   Instructor, Kyung Hee University, Seoul, Korea

## Publications

1. **Won, S.**, T. Ikegami, C. J. Peters, and S. Makino. 2007. NSm protein of Rift Vally fever virus suppresses virus-induced apoptosis. J. Virol. (In press)

2. Ikegami, T., **S. Won**, C.J. Peters, and S. Makino. 2007. Characterization of Rift Valley fever virus transcriptional terminations. J. Virol. 81: 8421-8438.

3. **Won, S.**, T. Ikegami, C. J. Peters, and S. Makino. 2006. NSm and 78-Kilodalton proteins of Rift Valley fever virus are nonessential for viral replication in cell culture. J. Virol. 80: 8274-8278.

4. Ikegami, T., **S. Won**, C.J. Peters, and S. Makino. 2006. Rescue of infectious Rift Valley fever virus entirely from cDNA, analysis of virus lacking NSs gene, and expression of a foreign gene. J. Virol. 80: 2933-2940.

5. Ikegami, T., **S. Won**, C.J. Peters, and S. Makino. 2005 Rift Valley fever virus NSs mRNA is transcribed from an incoming anti-viral-sense S RNA segment. J. Virol. 79: 12106-12111.

6. Nam, J., S. Chae, **S. Won**, E. Kim, K. Yoon, B. Kim, Y. Jeong, and H. Cho. 2001. Short report: Genetic heterogeneity of Japanese encephalitis virus assessed via analysis of the full-length genome sequence of a Korean isolate. Am. J. Trop. Med. Hyg. 65(4): 388-392.

## Summary of Dissertation

Rift Valley fever virus (RVFV) (genus *Phlebovirus*, family *Bunyaviridae*) has a tripartite negative-strand genome, causes a mosquito-borne disease that is endemic in sub-Saharan African countries and results in large epidemics among humans and livestock. Furthermore, it has potential as a bioterrorist agent and poses a risk for introduction to other areas. In spite of its danger, neither veterinary nor human vaccines are available. I established a T7 RNA polymerase-based reverse genetics system to rescue infectious clones of RVFV MP-12 strain entirely from cDNA, the first for any phleboviruses. Using this system, RVFV carrying substitution mutations of the M gene preglycoprotein region (pre-Gn region), one lacking NSm protein expression, one lacking 78-kDa protein expression, and one lacking expression of both proteins, were rescued and compared in cell culture. All of the mutants and their parent virus produced plaques with similar sizes and morphologies in Vero E6 cells and had similar growth kinetics in Vero, C6/36, and MRC5 cells, demonstrating that the NSm and 78-kDa proteins were not needed for the virus to replicate efficiently in cell culture. A competition-propagation assay revealed that the parental virus was slightly more fit than the mutant virus lacking expression of both proteins. To determine the biological functions of the NSm and 78-kDa proteins, I generated the mutant virus, arMP-12-del21/384, carrying a large deletion in the pre-Gn region of the M segment. Neither NSm nor the 78-kDa proteins were synthesized in arMP-12-del21/384-infected cells. Although arMP-del21/384 and its parental arMP-12 showed similar virus growth kinetics, viral RNA, and proteins accumulation in infected cells, arMP-12-del21/384 infection induced extensive cell death and produced larger plaques than did the arMP-12 infection. arMP-12-del21/384 replication triggered apoptosis, including caspase-3 activation, cleavage of its downstream substrate, poly-ADP-ribose polymerase, and activation of initiator caspases, caspase-8 and -9, early in infection as compared with arMP-12 replication. NSm expression in arMP-12-del21/384-infected cells suppressed the severity of caspase-3 activation. Further, NSm protein expression inhibited staurosporine-induced activation of caspase-8 and -9, demonstrating that other viral proteins were dispensable for the NSm's function in inhibiting apoptosis. RVFV NSm protein is the first identified Phleobovirus protein that has antiapoptotic function.

Permanent address:    114-602 Shin-il Utovil, Howon-dong, Uijeongbu, 480-917, Korea

This dissertation was typed by Sungyong Won.